rijksuniversiteit
groningen

# Masters Thesis

---

# Analysis and validation of a prototype activation mechanism for the Ocean Grazer

---


*Author*
H. (Hessel) K.J. Hartmans


Masters Research Project for Industrial
Engineering and Management

*Faculty of science and engineering*


*Supervisor*
prof. dr. A.I. (Antonis) Vakis

*Second supervisor*
drs. W.A. (Wout) Prins


November 11, 2021

# Abstract

This thesis aims to analyze the current design of the activation mechanism, and attain further insight into the functioning and efficiency of this mechanism. Moreover, provide advice for improvements and design of a final prototype activation mechanism when keeping efficiency, reliability, maintainability and robustness in mind.

Foremost, the design is structurally analyzed using manual computations and finite element method studies. The components are validated for robustness, strength, fatigue, and wear. The functionality of the activation is analyzed for its general working principle, its maintainability and a failure mode and effect analysis study is conducted to verify safety. Finally, for the analysis of efficiency, the losses in the bearings are computed, and a testing plan is drawn up for empirical validation of the energy losses of the system.

The results of the research show that all components of the activation mechanism are sufficiently strong with a significant margin, which is not usual for designing such mechanisms. The extra margin of strength is however useful to facilitate future upgrades and changes to the testing setup. The ratcheting function and the components which support this need to be tested for functionality empirically. The testing setup requires safety features to ensure the safety of humans and the testing setup. The losses are generated in principle by the bearings in the mechanism, this results in an efficiency of 98.64% - 99.93%. Finally, a testing plan is created for the empirical validation of the energy losses in the activation mechanism.

In closing, the activation mechanism is sufficiently robust, and well-designed for the testing setup. When the testing setup is assembled with the activation mechanism, certain safety measures need to be met. Thereafter, empirical testing is required in the future to verify the findings of this thesis. Future research will need to include the functioning of the ratcheting mechanism and a validation of the losses of energy in the system.

# *Acknowledgements*

During the time that I worked on the activation mechanism, many things changed. At first, the goal was to finish everything quickly so that the research would be ready for a funding proposal. However, due to changes in the planning of the Ocean Grazer company, the timeline for this project changed also. Initially, there was also the ambition to conduct more empirical tests, but due to the long production time of the components, this sadly was not possible. However, with the help and positive attitude of my supervisors and all members of the project group, the project has been a great experience.

The work that I have done would not have been possible without the help of my supervisors A.I. (Antonis) Vakis, and W.A. (Wout) Prins. Additionally, M. (Marijn) van Rooij has been instrumental in the process. They have guided me and the project in the right direction multiple times, and their contributions helped me understand the goal of this thesis, and also of the Ocean Grazer.

Moreover, I would like to thank the other students who are working on the Ocean Grazer. Weekly meetings and the social environment at the water hall have provided useful feedback and advice.

# Contents

**Abstract** i

**Acknowledgements** ii

**1 Introduction** 1
- 1.1 Renewable energy sources . . . 1
- 1.2 Ocean Grazer . . . 2
  - 1.2.1 Ocean Power . . . 2
  - 1.2.2 Company's goal . . . 3
  - 1.2.3 Research . . . 3
- 1.3 Purpose of the activation mechanism . . . 3
  - 1.3.1 Functioning of mechanism . . . 5
- 1.4 Components and features . . . 5
- 1.5 Research outline . . . 6

**2 Problem description** 7
- 2.1 Problem analysis . . . 7
- 2.2 System definition . . . 8
- 2.3 Stakeholder analysis . . . 9
- 2.4 Research goal . . . 10
- 2.5 Research questions . . . 10
- 2.6 Research methodology . . . 10

**3 Literature review** 11
- 3.1 Initial literature search . . . 11
- 3.2 Efficiency of mechanism . . . 11
- 3.3 Design for robustness, reliability, and maintainability . . . 12

**4 Research design** 13
- 4.1 Evaluation of design . . . 13
- 4.2 Key metrics of evaluation . . . 14
- 4.3 FEM software selection . . . 14
- 4.4 Tribological analysis . . . 15
- 4.5 Evaluation of efficiency . . . 15
- 4.6 Limitations of research plan . . . 15
  - 4.6.1 Dry testing . . . 15
  - 4.6.2 Wave generator . . . 15

**5 Structural analysis of prototype** 17
- 5.1 Loads on the system . . . 17
  - 5.1.1 Static loads . . . 17
  - 5.1.2 Inertial load at pickup . . . 18
  - 5.1.3 Total loads . . . 19

5.2 Structural analysis of components . . . 20
5.2.1 Axle . . . 20
Key slot in axle . . . 23
Fatigue analysis . . . 24
Important considerations when constructing axles . . . 24
5.2.2 Ratchet plate . . . 25
Fatigue analysis . . . 26
Wear rate . . . 26
Production difficulty . . . 27
5.2.3 Linear guide . . . 27
Linear flange detail analysis . . . 29
5.2.4 Pulleys . . . 29
5.3 Design recommendations . . . 30
5.3.1 Essence of structural analysis . . . 30
5.3.2 Design for reliability . . . 30

**6 Functional analysis** **31**
6.1 General working principle . . . 31
Method of activation . . . 31
One-way ratchet . . . 32
Angle of teeth . . . 32
6.2 Maintainability . . . 32
6.3 Safety . . . 33
6.3.1 Failure mode and effect analysis . . . 33
6.3.2 Required safety features . . . 34

**7 Efficiency analysis** **36**
7.1 Energy loss in the activation mechanism . . . 36
7.1.1 Scope . . . 36
7.1.2 Loss factors . . . 36
7.2 Required information . . . 37
7.2.1 Loss in bearings . . . 37
Total bearing loss . . . 38
7.3 Test plan . . . 38
7.3.1 Control variables . . . 39
7.3.2 Equipment . . . 39
Sensors . . . 39
Data acquisition . . . 40
7.4 Losses when submerged in viscous fluid . . . 40

**8 Discussion** **41**
8.1 Structural results . . . 41
8.2 Functional results . . . 42
8.3 Efficiency results . . . 42
8.4 Limitations . . . 43
8.5 Recommendations . . . 43
8.5.1 Design for robustness . . . 43
8.5.2 Design for maintainability . . . 43
8.5.3 Safety features . . . 44
8.6 Future work . . . 44

**9 Conclusion** **45**

**Bibliography** **46**

**A Shear and bending diagrams** **49**

**B FEM results of pulleys** **50**

**C Failure mode and effect analysis** **51**

**D Bearing types and coefficient of friction** **54**

# List of Figures

1.1 Global electricity demand by region in the Stated Policies Scenario, 2000-2040 [2]. . . . 1
1.2 Global electricity generation mix by scenario, 2018, Stated Policies and Sustainable Development Scenarios 2040 [4]. . . . 2
1.3 An artist impression of the Ocean Grazer, showing the structure above and below the water surface [5]. . . . 3
1.4 Photograph of three cylinders in the experimental setup. . . . 4
1.5 Schematic of location of the activation mechanism. . . . 4
1.6 Rendering of preliminary design of the activation mechanism. . . . 5
1.7 An illustration of the activation mechanism, showing the important components and features. . . . 6

2.1 3D render of the testing setup at the water hall of the University of Groningen. . . . 7
2.2 System description design, a schematic view of the mid-level system of a single pumping system in the Ocean Power system. . . . 8

4.1 Diagram of arm on the wave generator motor. . . . 15
4.2 A sum of three sinusoidal waves, resulting in an irregular and unpredictable wave [24]. . . . 16

5.1 3D rendering of all the rotating masses of the activation mechanism. . 19
5.2 Section view and free body diagram of all loads on the activation mechanism. . . . 19
5.3 Split up FBD in two sections. . . . 20
5.4 FEM results of study on the axle, where the shown stresses are above the 39.43 MPa which was calculated previously in Equation 5.16. . . . 22
5.5 FEM results of key way analysis with a maximum von Mises stress of 97.8MPa. . . . 23
5.6 FEM results of key way analysis with a flange component. The maximum von Mises stress in this study is 197.8 MPa. The iso-clipping image shows only stresses larger than 100 MPa. . . . 23
5.7 S-N curve of C45 steel, showing the bending stress in relation to the amount of loading cycles. (image credit: A. Lipski [26]) . . . 24
5.8 Ratcheting states. . . . 25
5.9 FEM study results of the ratchet plate where, in both cases, the von Mises stress does not exceed 3.2 MPa. The aluminum has a maximum deformation of 0.7$\mu m$ and the nylon has 28$\mu m$ of deformation. . . . 25
5.10 FEM analysis on a single tooth of the ratchet plate, with a maximum von Mises stress of 0.9 MPa. . . . 26
5.11 Image showing the curvature of the teeth. A lighter color represents a greater curvature, and a darker color represents a flatter surface. . . . 27
5.12 Von Mises stresses in the Linear flange. . . . 28

5.13 Elastic displacement in the linear guide assembly, where the largest displacement is 0.64 mm. . . . . 28
5.14 Linear flange FEM. . . . . 29

6.1 Ratchet plate teeth. . . . . 32

A.1 Diagrams of the axle computations. . . . . 49

B.1 FEM studies of the Dynamic- and floater pulley, showing the von Mises stress distribution. . . . . 50

# List of Tables

1.1 Combinations and area's of hydraulic cylinders. . . . . 3

5.1 Variables and Static loads of the system. . . . . 17
5.2 Static load and torque on the system. . . . . 18
5.3 Inertial load on the system resulting from pickup. . . . . 18

6.1 Scoring and actions. . . . . 34

7.1 Power loss in bearings. . . . . 38

C.1 FMEA worksheet. . . . . 51
C.2 Criteria for severity. . . . . 53
C.3 Criteria for Probability. . . . . 53
C.4 Criteria for Detection. . . . . 53

D.1 A table with the friction coefficients of different types of bearings. . . . 54

# List of Abbreviations

| | |
|---|---|
| **AM** | **A**ctivation **M**echanism |
| **BMD** | **B**ending **M**oment **D**iagram |
| **CM** | **C**orrective **M**aintenance |
| **DAQ** | **D**ata **Aq**uisition computer board |
| **DFR** | **D**esign **F**or **R**eliability |
| **ETA** | **E**vent **T**ree **A**nalysis |
| **FEM** | **F**inite **E**lement **A**nalysis |
| **FMEA** | **F**ailure **M**ode and **E**ffect **A**nalysis |
| **FOS** | **F**actor **O**f **S**afety |
| **HALT** | **H**ighly **A**ccelerated **L**ife **T**est |
| **HASS** | **H**ighly **A**cclererated **S**tress **S**creening |
| **HAST** | **H**ighly **A**ccelerated **S**tress **T**est |
| **IEA** | **I**nternational **E**nergy **A**gency |
| **MTBF** | **M**ean **T**ime **B**etween **F**ailures |
| **MTTF** | **M**ean **T**ime **T**o **F**ailure |
| **PHA** | **P**reliminairy **H**azard **A**nalysis |
| **PM** | **P**reventive **M**aintenance |
| **PSA** | **P**robabilistic **S**afety **A**ssessment |
| **RPA** | **R**isk **P**otential **A**ssessment |
| **RPN** | **R**isk **P**riority **N**umber |
| **SFD** | **S**hear **F**orce **D**iagram |

# Chapter 1

# Introduction

This first chapter aims to introduce and contextualize the need of wave energy harvesting devices and the need for technological solutions in this regard. The main stakeholder, the Ocean Grazer company, is also introduced and an outline of the research is presented.

## 1.1 Renewable energy sources

The worldwide demand for electric energy is growing fast (Figure 1.1), and the International Energy Agency (IEA) states that the demand is increasing by 2.1% every year until 2040. Furthermore, the IEA states that the demand for electricity is growing at double the rate of overall energy demand, where developing economies account for 90% of the growth of demand [1].

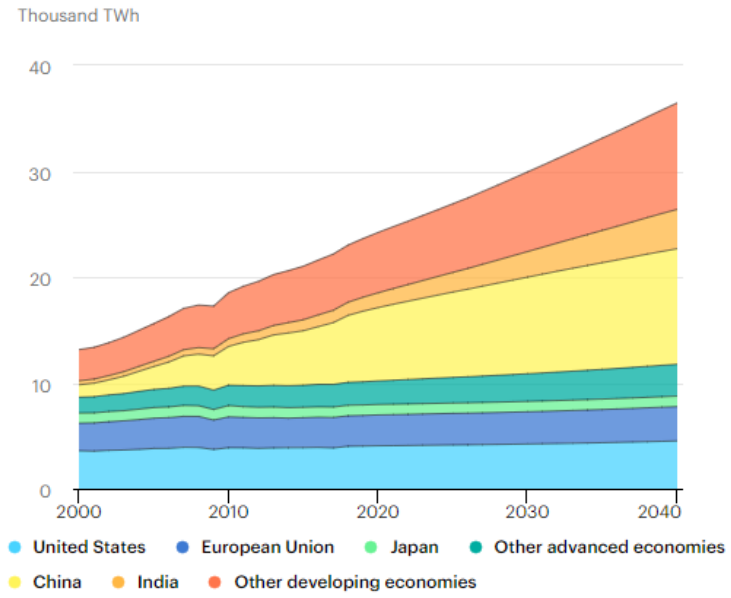


FIGURE 1.1: Global electricity demand by region in the Stated Policies Scenario, 2000-2040 [2].

The electricity that is currently being produced by can be seen in Figure 1.2, where currently more than half of the electricity that is being produced, is made with the use of non-renewable resources. The IEA state that the total investment in power until 2040 is expected to be $20 trillion. It is forecasted that by the year 2040, the production of electricity will be facilitated two thirds by renewable sources [1].

There are still many sources of energy that are not yet being used and are starting to gain traction, one of which is ocean energy. Energy that can be harvested in the ocean consists of two types, tidal- and wave energy. Initial studies show that the potential energy to be harvested is greater than the world's current energy consumption [3]. It is however not currently possible due to the underdeveloped harvesting technologies and economic and environmental problems that need solving first.

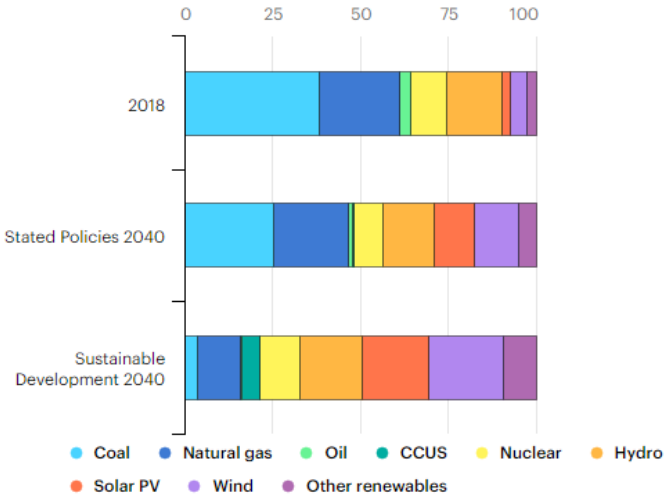


FIGURE 1.2: Global electricity generation mix by scenario, 2018, Stated Policies and Sustainable Development Scenarios 2040 [4].

## 1.2 Ocean Grazer

The Ocean Grazer is a Dutch startup company and a spinoff of the University of Groningen. The goal of the company is to create a wave-energy harvesting and storage device, which can be implemented worldwide. The "Ocean Power" project is a wave energy harvesting device that aims to extract energy from the ocean waves. The energy is subsequently stored in the "Ocean Battery" which is an underwater energy storage device. This device can store the abundance of energy when market demand is low, and release it when demand is high, providing the opportunity to never stop producing and limit overproduction.

### 1.2.1 Ocean Power

Ocean Power is the commercial name for the wave energy harvesting device. This device can generate electricity from waves with the use of floaters, that float on top of the surface of the waves. Figure 1.3 illustrates this system integrated into the ocean floor. The orange buoys floating around the main structure are the floaters which extract the energy from the waves, the whole floater structure is called the "floater blanket". The floaters pull on cables, which drives hydraulic pistons. The pressure difference created by these hydraulic pistons is stored in the Ocean Battery, this can then be converted into electrical energy with the use of turbines. The amount of energy which is extracted from the waves can be altered by coupling and decoupling the hydraulic cylinders, as well as altering the structure of the floater blanket.

FIGURE 1.3: An artist impression of the Ocean Grazer, showing the structure above and below the water surface [5].

### 1.2.2 Company's goal

The goal of the Ocean Grazer company is to:

*"bring wave power to maturity via synergy with existing technologies and the smart sharing of infrastructure"* [6].

### 1.2.3 Research

Presently, the team of the Ocean Grazer company is working together closely with the University of Groningen to develop fundamental knowledge. Knowledge is generated by creating underlying simulation- and mathematical models, together with testing prototypes. A fully working test setup is being built in the water hall facility at the University of Groningen, this set up can be used for experiments and iteration of components. The next phase of the project is to build a fully functioning prototype for full-scale ocean testing, so current research is focussed on gaining knowledge to facilitate this next step.

## 1.3 Purpose of the activation mechanism

The floater blanket above, on the surface, will pull on a cable which is attached to three hydraulic cylinders of different sizes. The areas of the pistons have been strategically chosen to represent area ratios of 1, 2 and 4 which can be seen in Figure 1.4.

The cylinders can be coupled in different combinations to create seven incremental steps of power generation, as more piston area results in a larger fluid displacement. The possible combinations are listed in Table 1.1.

TABLE 1.1: Combinations and area's of hydraulic cylinders.

| **Step** | **1** | **2** | **3** | **4** | **5** | **6** | **7** |
|---|---|---|---|---|---|---|---|
| Engaged Cylinders | 1 | 2 | 1,2 | 4 | 1,4 | 2,4 | 1,2,4 |
| Total area [$cm^2$] | 78.54 | 153.93 | 232.47 | 283.53 | 362.07 | 437.46 | 516 |

The subject of this thesis is the activation mechanism, which is the system that can couple and decouple each piston to the floater. Figure 1.5 shows a schematic


FIGURE 1.4: Photograph of three cylinders in the experimental setup.

where the activation mechanism is yellow. The activation mechanism needs to be able to activate and deactivate any piston when desired, switching pistons will occur in a timespan in the order of hours; therefore immediate activation is not necessary.

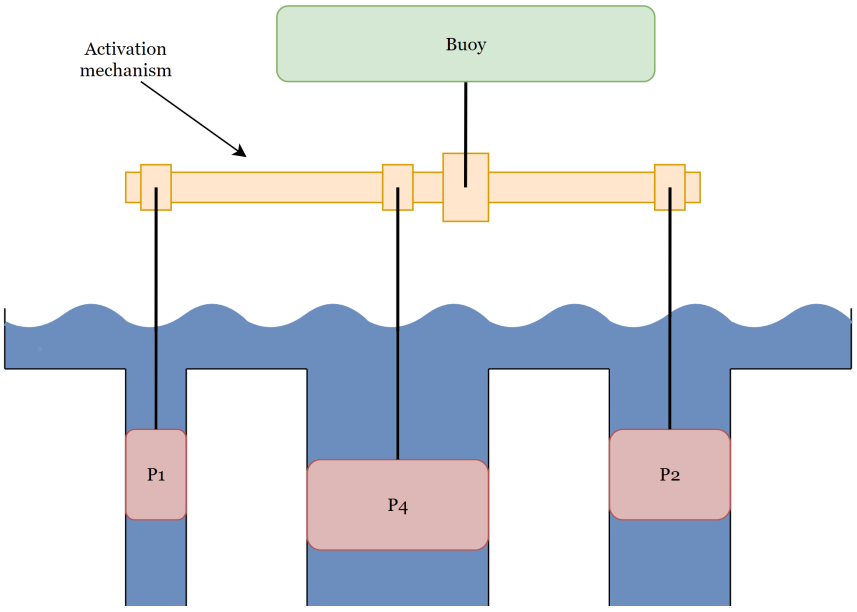


FIGURE 1.5: Schematic of location of the activation mechanism.

A preliminary design has been made for the experimental testing set up at the University of Groningen location. This design has been overdimensioned, and made to fit in the testing setup. This design is shown in Figure 1.6. This design can be used in the experimental setup for conducting tests on efficiency and functionality.

The focus of this thesis lies on analyzing this design of the activation mechanism. Moreover, providing efficiency data of the mechanism, and looking into improvements for the mechanism regarding the final implementation of the ocean prototype.

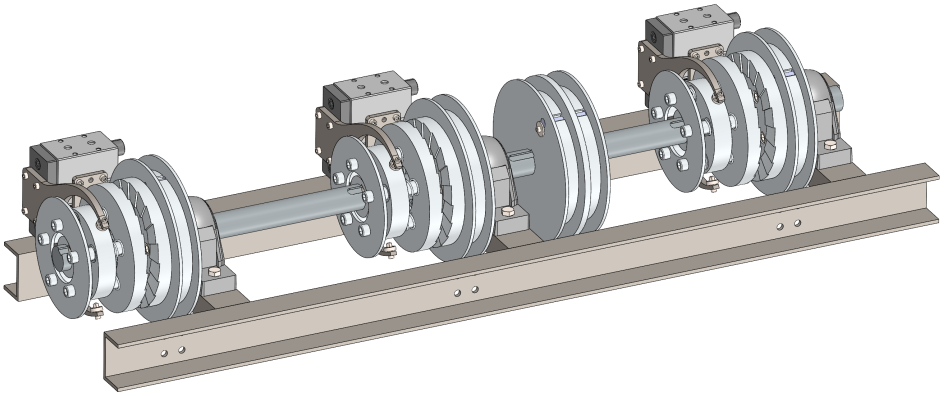

FIGURE 1.6: Rendering of preliminary design of the activation mechanism.

### 1.3.1 Functioning of mechanism

The activation mechanism should be able to independently control each piston, while in motion. A rattling mechanism much like a ratcheting wrench is needed in the system so that the piston is picked up every time at the lowest part of the wave.

The axle rotates back and forth in an oscillating motion with the movement of the waves, it is attached with a cable to the pulley second from the right. The three remaining pulleys can be coupled or decoupled to the axle by actuation of the pneumatic cylinders. Deactivation will leave them free to rotate on the axle, and the piston will be in its lowest position. When a cylinder needs to be activated, the pneumatic piston is disengaged and the rattling mechanism will engage the pulley. This allows the pulley to "rattle" in one direction, but is fixed in the other direction. When the floater is moving down, and the pistons are already in the lowest position in the cylinder, the rattling system allows the axle to rotate until the wave is at its lowest position. When the next wave picks up the floater, the axle will turn the other direction and pick the piston up at its lowest point. This ensures that the system functions at its highest possible capacity.

## 1.4 Components and features

This section discusses the most important components and features, which will be analyzed in this thesis. An overview of the main components is illustrated in Figure 1.7. The frame, is not shown and analyzed in this thesis because it will be constructed in an alternative method, outside the time scope of this project.

The **axle** is the main component, facilitating nearly all other components in the system. The axle is supported by the **main bearings**, which have a red color in the illustration. The **pneumatic cylinder** and the **actuation arm** function together as a lever which will disengage the ratchet mechanism and piston, both these components are colored blue in the illustration. When the pneumatic cylinder is actuated, the actuation arm is pushed against the **linear guide**. This subsequently pulls the **ratchet plate** through the **linear flange**, disengaging a piston. Every piston is mounted to a **dynamic pulley**, which can rotate freely on the axle, riding on bearings. The whole system receives power from the **floater pulley**, which is made with a double slot, to possibly facilitate a cable to pull the axle in the other direction. The floater pulley, and the linear flanges, are fixed from rotation on the axle using a **key slot**.

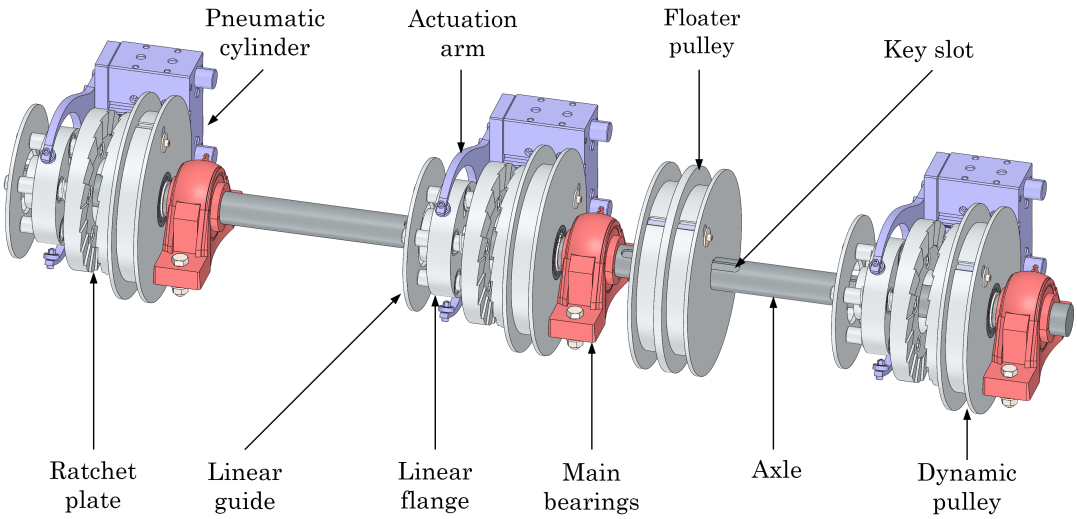


FIGURE 1.7: An illustration of the activation mechanism, showing the important components and features.

## 1.5 Research outline

The structure of this thesis is as follows, first the problem description (Chapter 2) analyzes the problem at hand, defining the scope and the direction of the research. Subsequently, the literature review (Chapter 3) discusses the work that has previously been done on this subject, and introduces some relevant topics for this thesis. The methodology is then drawn up in the research design (Chapter 4), discussing the methods and what needs to be analyzed.

The main research chapter of the thesis starts with the structural analysis of the prototype (Chapter 5), where all crucial components are structurally analyzed regarding the functioning of the system. The following chapter, the functional analysis, (Chapter 6) analyzes the functionality of the activation mechanism. Additionally, a safety analysis is performed. The final main chapter is the analysis of the efficiency (Chapter 7) where losses in the activation mechanism are identified and a plan for testing is drawn up.

The final chapters of the thesis begin with a discussion in Chapter 8. Additionally, in the discussion, the limitations of this thesis are mentioned. Finally, the thesis is concluded in Chapter 9, and the recommendations and future work is stated.

# Chapter 2

# Problem description

In this chapter of the thesis, the problem that was presented in the previous chapter is explored and analyzed, looking into the technical and engineering aspects of this research. Moreover, the problem is analyzed, and the goal is defined in accordance to the stakeholders' requirements.

## 2.1 Problem analysis

The first next big milestone for the Ocean Grazer project is a full-scale working prototype which can be implemented in the ocean for long-term testing. To achieve this, more knowledge is needed on many fronts of the project. A multiple of thesis have already been written about, or partially about, the activation mechanism by J. Welink [7], A. van Driel [8] and M. Abbas [9].

The testing setup at the water hall has been completely renewed, and will be the basis of the tests that are conducted in this thesis. The testing setup is made to have a high degree of modularity, so that parts and components can easily be substituted by alternative designs. This is an optimal setting for testing design iterations and conducting experiments. A 3D render of this setup is shown in Figure 2.1.

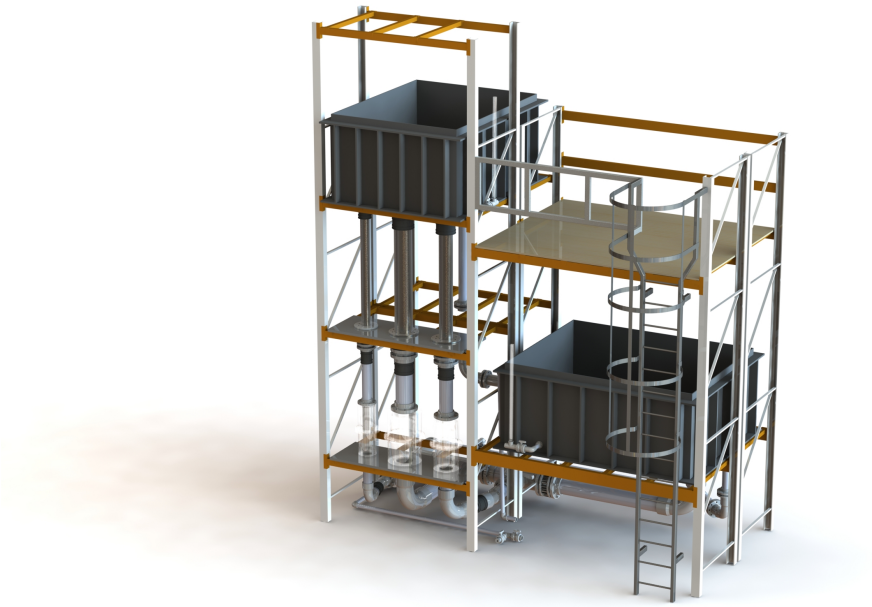

FIGURE 2.1: 3D render of the testing setup at the water hall of the University of Groningen.

The general goal of this thesis is to gather more critical information about the activation mechanism. This can be decomposed in the following important quality attributes.

- Efficiency
- Reliability
- Maintainability
- Robustness

These quality attributes are considered to be the key components of quality in the prototype version of the activation mechanism. The first important factor is its *efficiency*, being part of an energy harvesting system. One Ocean Power wave energy system is expected to have many activation mechanisms working side by side. The energy losses that are caused by this mechanical system must be kept to a minimum. The next important factor is its *reliability*. The prototype will be offshore and working in the ocean, therefore harder to maintain. This calls for a mechanism with a high reliability. Parts and mechanisms must be designed in a manner such that the working life is as long as possible. Furthermore, if a part or subassembly does break and stops working, it will need to be repaired out in the ocean. This leads to the next important quality attribute, which is *maintainability*. The final attribute can also be related to the reliability, which is that the system needs to have high degree of *robustness*. This is important in the case where the forces on the system exceed those of the use case. A good example for this is a storm, where the system is put under unusual loads not seen in normal functioning.

## 2.2 System definition

The "Ocean Power" system works with a large floater blanket, which consists of many individual buoys. Each separate buoy is connected to a system which is described as the mid-level system in Figure 2.2. Therefore, in reality, the higher level system consists of multiple mid-level systems working in parallel.

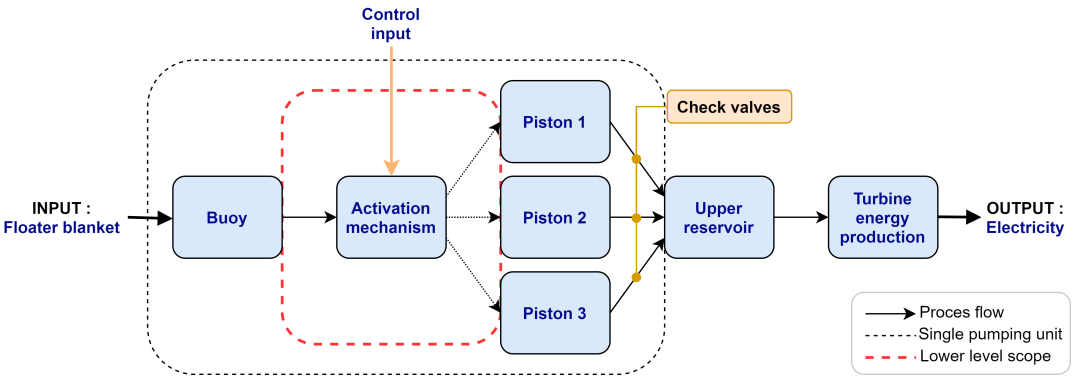


FIGURE 2.2: System description design, a schematic view of the mid-level system of a single pumping system in the Ocean Power system.

The system that is described in this paragraph zooms in to the mid-level system in Figure 2.2. The floater blanket will have many buoys that are all interconnected, providing energy to a pumping system. The buoys generate a vertical linear oscillating motion, which is provided from the waves. This motion is selectively transferred to the different pistons with use of the activation mechanism. The pistons pull the

liquid through check valves at the bottom of the cylinder, which make sure the liquid does not flow back down. The check valves are included in the system description because they are responsible for energy losses shown by research of L. Hut [10]. The activation mechanism is controlled from an outside source, and by predicting and analyzing the waves' amplitude and frequency. Larger waves will cause the activation of a larger pumping volume, and smaller waves vice versa. The liquid is pumped to a higher elevation and thus creates potential energy. This energy can be converted into electricity with the use of hydro-turbines.

This thesis zooms in on a single pumping system, and considers only the contents of the Red dotted box of Figure 2.2, which is the lower level system. The input of this system is a vertical linear oscillating motion, and the output is selectively actuated pistons in the same vertical linear oscillating motion. The pistons that are in a deactivated state rests in a stationary position in the bottom of its cylinder. Conversely, the other components in the system will be part of the efficiency analysis of the system.

## 2.3 Stakeholder analysis

The stakeholders of this project are divided into two groups that are the direct- and the indirect stakeholders. The direct stakeholders have a direct effect or are directly affected by this project. The indirect stakeholders are indirectly affected by this project.

**Direct stakeholders**

- **Drs. W.A. Prins** (Problem owner): Drs. Prins is the inventor of this system and serves as a Scientific advisor. He is working closely together with the research and also works on the company side of the Ocean Grazer. Moreover, Drs. Prins is the second supervisor of this thesis.
- **Prof. dr. A.I. Vakis** Works as a scientific advisor for the research of the project and is also taking the lead on the writing of the scientific papers. Moreover, he is the first supervisor of this thesis, and he is the Chair of the Computational Mechanical and Materials Engineering (CMME) research group. This is the group under which this thesis is written.
- **MSc. M. van Rooij** is the CTO of the Ocean Grazer company, and is closely involved in the design and testing of all components. MSc. van Rooij will take the lead on the development of the real size prototype, for testing in the ocean.
- **Ocean Grazer company** is financially involved in this research, and will receive insight and knowledge on how to reach their long-term goal of harvesting energy from the waves.
- **University of Groningen** provides scientific advice and knowledge to the Ocean Grazer group. Furthermore, the University of Groningen provides research students and financial support.

**Indirect stakeholders**

- **Researchers of the OG.** Previous, current and future researchers that are working on the Ocean Grazer project. The research of this thesis is built upon that

of what has been done in the past, and will contribute to the students that will conduct research in the future.

## 2.4 Research goal

The goal for this thesis is formulated to help guide the direction of research and lay the groundwork for the methodology. The goal is stated as:

*"To analyze the current design of the activation mechanism, and attain further insight into the functioning and efficiency of this mechanism. Moreover, provide advice for improvements and design of a final prototype activation mechanism when keeping efficiency, reliability, maintainability, and robustness in mind."*

The deliverable for this project will be a report and setup that satisfies this goal.

## 2.5 Research questions

Research questions are formulated with the aim of reaching the deliverable in an efficient and timely manner. The main research question is stated as:

*"What are the critical points of the activation mechanism, and what improvements can be made to the current design for testing a final prototype in the ocean?"*

To support the research in moving towards answering the main research question, sub-questions are formulated:

- *How can the activation mechanism be analyzed and tested?*
- *What are the efficiency losses in the activation mechanism?*
- *What are the critical points at each stage of activation?*
- *Which design parameters can be altered to improve the mechanism in its reliability, maintainability and robustness?*

## 2.6 Research methodology

The first step in this research is to conduct a literature analysis. With this first step, the goal is to gather information on rattling mechanisms, and the activation thereof. Moreover, to find information on designing offshore mechanisms with the goal of reliability and maintainability.

The next step is to build a testing set up where different components can be tested and the functionality of the mechanism can be analyzed. Here, all stages of activation and deactivation are evaluated, and the critical points are evaluated. A further step in this stage is to add sensors to the mechanism, and evaluate it for efficiency and energy losses.

Finally, if required, redesign, FEM studies, and tribological analysis will be conducted for critical components.

# Chapter 3

# Literature review

This chapter presents the research that has previously been done on the activation mechanism and the literature that is relevant to the topic of research.

## 3.1 Initial literature search

The activation mechanism is not new, and a multiple of thesis have already been written on the subject. The first thesis by J. Welink [7] is about creating a scale model of the Ocean Grazer. A small section of his research covers a scale model of the activation mechanism. Later, M. Abbas [9] created a proof of concept version of the AM, with a radial ratchet mechanism. Simultaneously, L.J.P. Evers [11] wrote a master's thesis on the design of a transmission mechanism for the Ocean Grazer. This is now known as the activation mechanism. The most recent thesis was written by A. van Driel [8], which focuses on designing the final AM in full scale for deployment in the ocean.

The following literature is focussed on similar ratchet mechanisms and on FEM studies on journal bearings. First, V.P. Bondaletov [12], presents research on a ratchet mechanism in transmissions. This research is, however, focussed on a ratchet mechanism which is not directly comparable to the current design. The research of T.J. Mackin et al. [13] is more comparable to the geometry of the ratchet plates of the AM. This research evaluates the fatigue failure life of a star-ratchet gear in bicycles. Finally, P.K. Goenka [14] describes how to conduct a viable FEM analysis on journal bearings.

## 3.2 Efficiency of mechanism

For the Ocean Grazer project, it is of high importance to have an accurate indication of the energy losses and efficiency of the AM. The main losses of the system are expected to be caused by the bearings. V. Bakolas et al. [15] have done research on the approximation of the global energy consumption of ball bearings. In the research, losses in ball bearings are specifically discussed. Moreover, the research of S. Iqbal et al. [16] focuses on finding the power loss in needle roller bearings. Finally, regarding the ratcheting mechanism, C. Jarzynski and O. Mazonka [17] attempt to make a solvable model of a ratchet and pawl system. While not the same ratcheting mechanism is described here, the theory could be useful.

## 3.3 Design for robustness, reliability, and maintainability

The final design of the activation mechanism is for an offshore application, and constructing components for a rough environment brings a need for additional considerations. The following sources can act as aid when designing or robustness, reliability and maintainability.

For constructing machine parts like the ratchet plate, the Roloff/Matek books by D. Jannasch et al. [18] [19] provide helpful tables and fundamental knowledge about gears and axles. Additional knowledge on designing components for reliability is found in the book: "Design for reliability" of D. Crowe and A. Feinberg [20]. W. Mulder et al. [21] provide guidelines for designing for maintainability, reliability, and supportability. Finally, the research of J. Smith and P.J. Clarkson [22] describes a method of assessing the robustness of mechanical designs.

For the ratcheting mechanism in the AM, the research described above of T.J. Mackin[13] provides essential knowledge about the construction of a radial star shaped ratchet gear. Additionally, for the potential diagnosis of the ratchet mechanism, B. Polok and P. Bilski [23] describe a method for diagnosing a bicycle ratchet mechanism using acoustics.

# Chapter 4

# Research design

The first step to conducting research on the activation mechanism is to build a basis for testing. The setup up is being built with a high degree of modularity. Because of this, components can be easily switched out if they are broken or for testing new configurations.

There are two stages to the research of this thesis, the first is to analyze the working activation mechanism, evaluate its weak components, and identify the critical points in each step of the activation process. This will be further explained in section 4.1. The next step is to evaluate the efficiency of the system and its subcomponents. Sensors will be added in different locations and components can be switched out to isolate and evaluate the system or subsystem. This is explained in Section 4.5. Finally, if necessary, a FEM and Tribological analysis will be conducted to improve components of the activation mechanism.

## 4.1 Evaluation of design

This part of the research will focus on the activation mechanism and its components. Each component will be evaluated in the four important requirements stated in Section 2.1: efficiency, reliability, maintainability, and robustness. The activation mechanism has five states of activation, each with possibly different critical points. They are described below.

- **State 1: All three pistons deactivated.** In this state, the main axle is rotating back and forth, but the pistons are deactivated and sitting in their resting positions. The resting positions are when the pulleys are fully unrolled and the pistons are sitting in the bottom most point of the cylinders.
- **State 2: Activation of a piston, or multiple pistons.** This state is the moment at which the ratcheting mechanism is engaged, fixing the pulley to the main axle in one direction. When the axle rotates the other direction, it will cause the ratchet to rattle and lower the engagement point. This state therefore concerns its self with the vulnerabilities regarding the actual activation of the ratchet.
- **State 3: Any combination of pistons in the activated state.** This state is when any combination of the three pistons (as shown in Table 1.1) are engaged. Every single combination has different forces acting upon it in different places.
- **State 4: Rattling of the mechanism.** This concerns the rattling of the ratcheting mechanism and the robustness and tribological phenomena thereof. Furthermore, the teeth of the ratcheting mechanism and their durability.

- **State 5: Deactivation of a piston, or multiple pistons.** This state is the moment at which the ratcheting mechanisms are disengaged and the pistons are allowed to rest in their resting positions.

The different states are to be evaluated by observation and testing. This includes switching between the states, different waves as input, and observing the changes in function or wear of the components.

## 4.2 Key metrics of evaluation

When evaluating the critical points of each state of activation, there are relevant key metrics to observe. Every state of activation exhibits different relevant artifacts. Not all metrics apply to every state. The key metrics that are listed below are based on what is estimated to be a critical component in the system.

**State 1:** This state is fully deactivated, and only experiences wear on the main bearings, the bearings in the pulleys, and the bearings that deactivate the ratcheting mechanism. The bearings and running surface should be evaluated and validated for the given loads.

**State 2:** Here, the teeth of the ratchet are subject to wear and impacts. While the teeth are engaged, there is a possibility of impact on the teeth. The severity of these impacts are to be evaluated analytically, and a FEM study should be conducted to validate and dimension the teeth. Moreover, this state includes the functioning of the pneumatic actuator and the components being actuated.

**State 3:** Each combination of active pistons in the system will lead to a distinct distribution of loads on the system. Moreover, there is a torsional load on the linear guide that facilitates the ratcheting function. These stresses in the components as a result of these different loads need to be analyzed. The axle will be evaluated and dimensioned for the maximum load case. The linear guide has been designed in this testing prototype without regard for load and friction. Therefore, the linear guide will have to be validated for its use case.

**State 4:** While rattling, the teeth slide against each other, this has the potential to cause wear on the surfaces. To measure the effects of wear, the height of the teeth will be carefully measured before and after testing. This can be combined with wear calculations to determine the wear rate and life of the ratchets.

**State 5:** This state exhibits forces on the activation plate that otherwise are not present in the other states. The components that are involved in the actual activation of the mechanism are to be validated.

## 4.3 FEM software selection

As stated in subsection 4.2, some components of the system will need to be analyzed using the Finite Element Method. The software that will be used for doing FEM analysis is SolidWorks. This software is chosen because of its integration in a design environment. This research has a practical application with a focus on improving

this mechanism. SolidWorks Has tools with which the design of components can be efficiently iterated based on results from FEM studies.

## 4.4 Tribological analysis

The running surfaces that exist in the mechanism are the ratchet plates. These have surfaces to surface sliding contact. To evaluate the components for testing purposes, the wear should be calculated in the worst-case scenario.

## 4.5 Evaluation of efficiency

An important metric for the Ocean Grazer project is to have knowledge of the losses in the whole system, and how they originate. The design needs to be evaluated for energy losses and what the origin of the loss is. A testing plan needs to be written which contains the tests that need to be done, and how the tests are to take place.

## 4.6 Limitations of research plan

This section lists and described the main limitations of the research that is being conducted in this thesis. Moreover, the consequences of the limitations are explained.

### 4.6.1 Dry testing

This setup is built for testing above water, where the system stays dry and therefore is isolated from the corrosional and frictional effects of being surrounded by a liquid. The prototype will require the activation mechanism to be submerged in the hydraulic liquid, presumably leading to an additional efficiency loss and increased corrosion.

### 4.6.2 Wave generator

Currently, at the testing facility, there is an electric motor with a gearbox that produces the wave function. On the shaft of the motor an arm is attached, on which the floater cable can be mounted. This arm can be seen in Figure 4.1. Attaching the floater cable at different distances from the center, will change the wave height. Changing the angular velocity of the motor varies the wave period. The combination of changing these two variables can simulate regular sinusoidal waves with a period in the range of 5 to 100 seconds, and an amplitude of 200 to 600 millimeters. This amplitude is equal to vertical displacement of the pistons between 400 and 1200 millimeters.

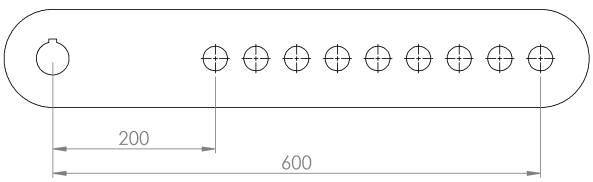


FIGURE 4.1: Diagram of arm on the wave generator motor.

The ocean, however, rarely exhibits perfect regular sinusoidal waves. Real situations are more often referred to as the "random sea", showing irregular waves, with different height, length, and direction [24]. The ocean's irregular wave patterns are, in most cases, composed of a multiple of regular sinusoidal waves. Figure 4.2 shows an irregular wave $\zeta_1 + \zeta_2 + \zeta_3$ which can be decomposed into the waves $\zeta_1$, $\zeta_2$ and $\zeta_3$.

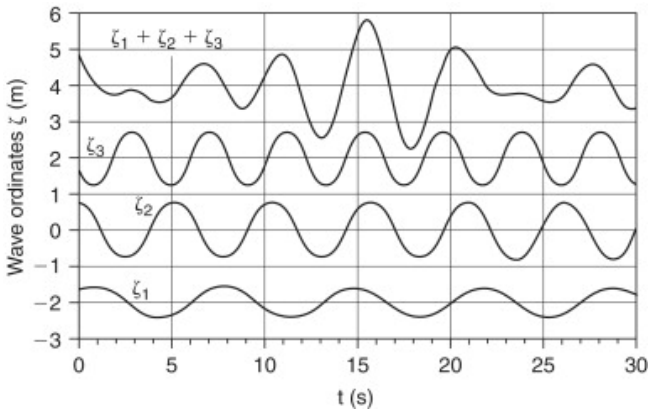


FIGURE 4.2: A sum of three sinusoidal waves, resulting in an irregular and unpredictable wave [24].

However, due to the current controller of the motor, not possible to simulate irregular or asymmetrical waves. In future research, it can be desirable to replace the electric motor by a linear actuator. This will enable the setup to test irregular and asymmetric waves.

# Chapter 5

# Structural analysis of prototype

This chapter has the aim of validating the design of the prototype and analyzing the if the mechanism is structurally acceptable. First, the static loads and torques on the system will be determined, thereafter the effects of inertial loads are calculated. This chapter should provide and discuss all forces acting on the activation mechanism, to serve as groundwork for stress and structural analysis.

## 5.1 Loads on the system

First the loads on the system need to be determined, forces can be determined from the area of each piston and the maximum water column that is possible in the testing setup. The loads are determined in the worst-case scenarios that in the system. There are additional forces which are caused by the friction interface between the pistons and cylinders, this interface will not be included as the pistons have not been evaluated for this.

### 5.1.1 Static loads

The maximum column of water which can stand on the pistons in their lowermost position is 2844 mm, which is rounded up to 3 m. The three pistons of the test setup have diameters of 100, 140 and 190 millimeters. Using the pressure and area relationship, the force of the water column on the pistons can be calculated with

$$F_{wc} = r^2 \pi \, H_c \rho_w g \tag{5.1}$$

where $r$ is the radius of the pistons $(m)$, $H_c$ is the height of the water column $(m)$, $\rho_w$ is the density of water $(kg/m^3)$ and $g$ is the gravitational acceleration $(9.81 \; m/s^2)$. The force of the water column and the weight of the pistons add up to the total static loads on the pistons and is shown in table 5.1.

TABLE 5.1: Variables and Static loads of the system.

| | Diameter ($d$) | Area ($A$) | Water load ($F_{wc}$) | Piston weight ($M_p$) | Total static load ($F_s$) |
|---|---|---|---|---|---|
| Piston A | 0.19 $m$ | 0.028353 $m^2$ | 834 $N$ | 25.5 $kg$ | 1085 $N$ |
| Piston B | 0.14 $m$ | 0.015393 $m^2$ | 453 $N$ | 12.7 $kg$ | 578 $N$ |
| Piston C | 0.1 $m$ | 0.007854 $m^2$ | 231 $N$ | 6.1 $kg$ | 291 $N$ |
| TOTAL | | | 1518 $N$ | 44.3 $kg$ | 1954 $N$ |

Furthermore, a multiple of torques act on the system, the pulleys of the activation mechanism have a diameter of 210 mm. Due to the rolling up of the cable on the pulley, the diameter can increase. To account for this effect, the diameter which is used to calculate the torque on the axle is rounded up to 230 mm. This diameter

is used to compute the torque on the axle at the piston-specific locations, shown in table 5.2. The total static load and static torque are forces which act on the floater pulley, as this pulley balances the forces of all the pistons.

TABLE 5.2: Static load and torque on the system.

| | Static load ($F_s$) | Static torque ($\tau$) |
|---|---|---|
| Piston A | 1085 $N$ | 95.9 $Nm$ |
| Piston B | 578 $N$ | 52.1 $Nm$ |
| Piston C | 291 $N$ | 26.6 $Nm$ |
| TOTAL | 1954 $N$ | 175.6 $Nm$ |

### 5.1.2 Inertial load at pickup

When picking up pistons from the bottom of the cylinders, this adds a load on the system, namely the inertial pickup load. This is the force incurred on the system due to the acceleration of a mass. Concerning this prototype, there are the moments of inertia in the water column, pistons and the angular moment of inertia of the axle.

First, the linear acceleration that is possible needs to be determined. The maximum acceleration of the pistons upwards is a result of the capabilities of the wave generator mentioned in Subsection 4.6.2. The largest acceleration will occur when the largest amplitude, and shortest period are chosen in testing. The current setup of the wave generator allows for an amplitude of 0.6 meters and a period of 5 seconds. The linear acceleration of the pistons is equal to the centripetal acceleration, which can be calculated with

$$a_c = r\omega^2 \tag{5.2}$$

where $r$ is the radius of the rotating point $(m)$, and $\omega$ is the angular velocity of the rotation $(rad/s)$. The angular velocity of the wave generator with a period of 5 seconds is 1.26 $rad/s$, the radius is 0.6 meters. This results in a linear acceleration of 0.95 $m/s^2$. In the research of A. van Driel it is mentioned that the acceleration function of waves reaches a maximum of 0.82 $m/s^2$, this is comparable to the acceleration that the wave generator can produce [8]. The acceleration will be rounded up to 1 $m/s^2$, to account for error and provide the possibility of actuator upgrades in the future. The loads due to linear acceleration of the masses can be calculated with

$$F_i = (m_w + m_p)a_{pickup} \tag{5.3}$$

where $m_w$ is the mass of the water columns $(kg)$, $m_p$ is the mass of the pistons $(kg)$ and $a_{pickup}$ is the linear acceleration $(m/s^2)$. Table 5.3 summarizes the inertial loads on the system due to the acceleration of the water column and the pistons.

TABLE 5.3: Inertial load on the system resulting from pickup.

| | Water column weight ($m_{wc}$) | Piston weight ($m_p$) | Inertial load ($F_{li}$) |
|---|---|---|---|
| Piston A | 85.0 $kg$ | 25.5 $kg$ | 110.5 $N$ |
| Piston B | 46.2 $kg$ | 12.7 $kg$ | 58.9 $N$ |
| Piston C | 23.6 $kg$ | 6.1 $kg$ | 29.7 $N$ |
| TOTAL | 154.6 $kg$ | 44.3 $kg$ | 198.9 $N$ |

Another inertial load is the rotational inertia of the activation mechanism. All the rotating parts are isolated in SolidWorks, which can be seen in Figure 5.5. The

moment of inertia around the Z axis can be derived from SolidWorks when defining all the correct materials and masses, and is 0.323 $kg\,m^2$.

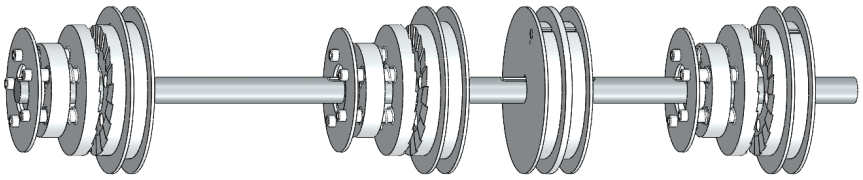

FIGURE 5.1: 3D rendering of all the rotating masses of the activation mechanism.

The load on the system as a result of the rotational inertia acts on the floater pulley. This is the driving pulley that sets everything in motion. The load is in the form of torque, and can be determined with

$$T = I_r \left( \frac{a_{tangential}}{r} \right) \tag{5.4}$$

where $I_r$ is the moment of inertia of the rotating masses $(kg\,m^2)$, $a_{tantential}$ is the linear acceleration $(m/s^2)$, and $r$ is the radius of the pulley $(m)$. The term between the brackets converts linear acceleration to angular acceleration $(rad/s^2)$. The total torque as a result of the rotational inertia, using Equation 5.4 equals 30.8 Nm.

### 5.1.3 Total loads

The first load to take in to consideration is the mass of the activation mechanism itself. The axle has a mass of 13.2 kg, the individual actuation mechanisms have a mass of 7.6 kg and the floater pulley has a mass of 7.7 kg. These masses are converted to forces, and act on the location of the centers of the pulleys. All forces are summed up, and shown in Figure 5.2, where the section view illustrates the location of the forces on the mechanism.

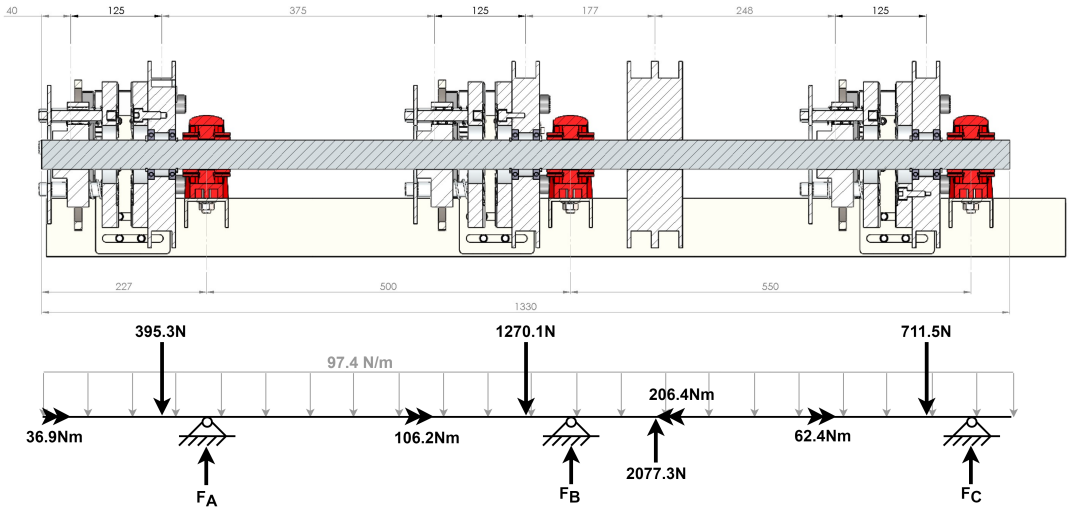


FIGURE 5.2: Section view and free body diagram of all loads on the activation mechanism.

## 5.2 Structural analysis of components

### 5.2.1 Axle

Before stress in the axle can be calculated, the reaction forces of in all the supports need to be determined, this can be done with using two equations of equilibrium. Namely,

$$\sum M_i = 0 \tag{5.5}$$

$$\sum F_y = 0 \tag{5.6}$$

where Equation 5.5 is the sum of moments, around the support points A, B and C. Equation 5.6 is the sum of forced in the y-axis direction. To use these equations, the beam is split up into two sections, and each is computed separately. The free body diagram from Figure 5.2, is split up into the two beams below, shown in Figure 5.3.

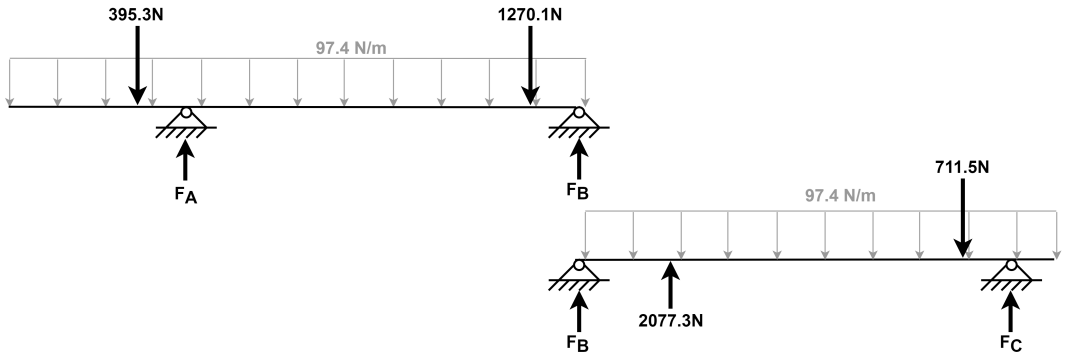


FIGURE 5.3: Split up FBD in two sections.

The reaction forces are found to be $F_A = 644.4N$, $F_B = -448N$ and $F_C = 223.8N$. With all forces and reaction forces now known, the shear force across the axle can be found using

$$V(x) = \int w(x)dx \tag{5.7}$$

where $V(x)$ is the shear force $(N)$ relating to the position on the axle, and $w(x)$ is the load distribution $(N/m)$ in relation to position on the axle. A diagram (Appendix A, Figure A.1a) can be made that shows the variation of shear force across the axle, this is called the shear force diagram (SFD).The highest shear force that exists in the axle is $V(N) = 1547.11N$.

The shear force can be integrated to find the bending moment in the axle, this can be accomplished using

$$M(x) = \int V(x)dx \tag{5.8}$$

where $M(x)$ is the bending moment $(Nm)$ in relation to the position on the axle, and $V(x)$ is the shear force $(N)$ in relation to the position on the axle. The result of this can be plotted to create a bending moment diagram (BMD), which is shown in Appendix A, Figure A.1b.

After finding the shear force, bending moment and turning moment, the stresses in the shaft need to be analyzed. There are three different loading types in this case,

each of which generates a different stress. These stresses are axial stress, torsional stress and bending stress, which are defined respectively as,

$$\sigma_a = \frac{P}{A} \tag{5.9}$$

$$\tau = \frac{Tr}{J} \tag{5.10}$$

$$\sigma_b = \frac{My}{I} \tag{5.11}$$

where in Equation 5.9 $P$ is the axial load $(N)$, and $A$ is the cross-sectional area $(m)$. In Equation 5.10 $T$ is defined as torque $(Nm)$, $r$ is the radius $(m)$ and $J$ is the polar moment of inertia $(m^4)$. In Equation 5.11, $M$ is the bending moment $(Nm)$, $y$ is the extreme fiber distance from the neutral axis $(m)$ and $I$ is the moment of inertia $(m^4)$. Regarding a solid, round bar, the polar moment of inertia and moment of inertia can be found respectively using:

$$J = \frac{\pi d^4}{32} \tag{5.12}$$

$$I = \frac{\pi d^4}{64} \tag{5.13}$$

The maximum torque and bending moment in the axle can be found from Figure A.1b. The maximum torque in the axle is 143.1 Nm and the maximum bending moment is -179 Nm. The torsional stress and bending moment in the shaft are found respectively with,

$$\tau = \frac{Tr}{J} = \frac{32Tr}{\pi d^4} = \frac{32 \cdot 143.1 \cdot 0.01875}{\pi \left(0.0375\right)^4} = 13.82MPa \tag{5.14}$$

$$\sigma_{b_y} = \frac{My}{I} = \frac{64My}{\pi d^4} = \frac{64 \cdot -179 \cdot 0.01875}{\pi \left(0.0375\right)^4} = -34.58MPa \tag{5.15}$$

Using these two stresses, the principal stress can be found. This is the maximum and minimum stress on a plane where there is no shear stress present. The values are found using the following equation,

$$\sigma_{1,2} = \frac{\sigma_x + \sigma_y}{2} \pm \sqrt{\left(\frac{\sigma_x - \sigma_y}{2}\right)^2 + \tau^2} = \frac{0 - 34.58}{2} \pm \sqrt{\left(\frac{0 + 34.58}{2}\right)^2 + (13.82)^2} \tag{5.16}$$

The maximum stress is 4.84 MPa and the minimum stress is -39.43 MPa. To validate these stresses in the axle, the maximum allowable stress of the axles material needs to be determined. The axle is made from C45 steel. From table 1-1 in Roloff/Matek [19], the permanent elongation 0.2% for C45 steel is $R_{p0.2N} = 500N/mm^2$. Additionally, the stress concentration factor is found in table 3-11, this is $K_t = 0.955$. The allowable bending and shear stress is then calculated with,

$$\sigma_y = 1.2 \cdot R_{p0.2N} \cdot K_t = 1.2 \cdot 500 \cdot 0.955 = 572MPa \tag{5.17}$$

$$\tau_t = \frac{1.2 \cdot R_{p0.2N} \cdot K_t}{\sqrt{3}} = 1.2 \cdot 500 \cdot 0.955 = 330.8MPa \tag{5.18}$$

From this, the safety factor in the axle is:

$$FoS = \frac{1}{\sqrt{\left(\frac{\sigma_{bmax}}{\sigma_y}\right)^2 + \left(\frac{\tau_{tmax}}{\tau_t}\right)^2}} = \frac{1}{\sqrt{\left(\frac{-39.43}{572}\right)^2 + \left(\frac{13.82}{330.8}\right)^2}} = 12.4 \tag{5.19}$$

A safety factor of 12.4 is found, which is considered to be high. The minimum safety factor for an application like this is 1.5. However, due to the prototyping environment, additional strength can be desirable for future changes to the system. Furthermore, because there is a linear motion guide on the axle in the axial direction, any deformation is undesirable. Maximum deformation of the axle in the worst case is found with,

$$\delta_{max} = \frac{-Pba}{6EIL}\left(L^2 - b^2 - a^2\right) \tag{5.20}$$

$$= \frac{-2077.3 \cdot 0.435 \cdot 0.115}{6 \cdot 190x10^9 \cdot 9.71x10^{-8} \cdot 0.55}\left(0.55^2 - 0.435^2 - 0.115^2\right) = -0.171mm \tag{5.21}$$

where $P$ is the load $(N)$, $b$ and $a$ are the distances to the bearings $(m)$, $E$ is the modulus of elasticity $(Pa)$, $I$ is the moment of inertia $(m^4)$ which is found with Equation 5.13, and $L$ is the distance between the bearings $(m)$. The maximum deflection of the axle which is seen is -0.171 mm. This is the part of the axle where the floater pulley is mounted between the two most right bearings of Figure 5.2. For future calculations, it is important to look at the deformation of the axle at all points, to verify the movement of each piston due to deformation of the AM.

For redundancy, a FEM study is done on the axle. The results of the study are shown in Figure 5.4. The only stresses shown in the Figure are the stresses larger than 39.43 MPa, which is what the manual calculation resulted in (Equation 5.16). The results of the FEM study and the manual calculation show similar results in bending stress and deformation. The manual calculation was, however, conducted on the smallest geometry seen on the axle: 37.5 mm. This is the reason why the results of the two cannot be compared equally. The FEM study does show, however, that there is are potential higher stresses in the key way. This will be further analyzed in the forthcoming sections.

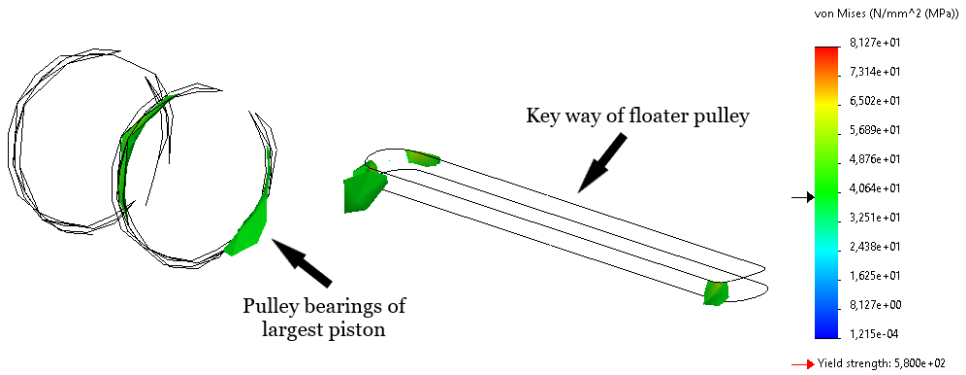


FIGURE 5.4: FEM results of study on the axle, where the shown stresses are above the 39.43 MPa which was calculated previously in Equation 5.16.

### Key slot in axle

The axle requires key ways to transfer the torque of the pulleys into the axle and other components. The key way size is validated with a FEM analysis. A torque of 206.4Nm is the largest acting torque on a key way, and equals a force of 5160 N on the face of the key of a 40 mm axle. The key is made of AISI304 chromium-nickel stainless steel.

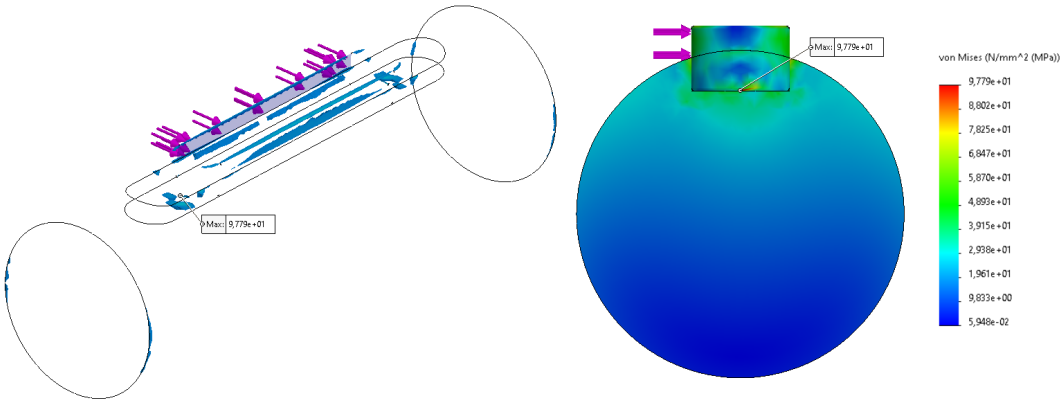


FIGURE 5.5: FEM results of key way analysis with a maximum von Mises stress of 97.8MPa.

Another FEM study was conducted where the linear flange is added to the assembly. The linear flange is one of the components that needs to transfer torque to and from the axle using a key. The axle, key and flange have been entered in the software to have global contact, meaning that the components are not bonded, but also allow no penetration. This closely resembles the real-world situation with an axle and key way. Figure 5.6 shows the results of the study, with a maximum von Mises stress of 197.8 MPa. This stress is solely present in the edge of the key way in the axle.

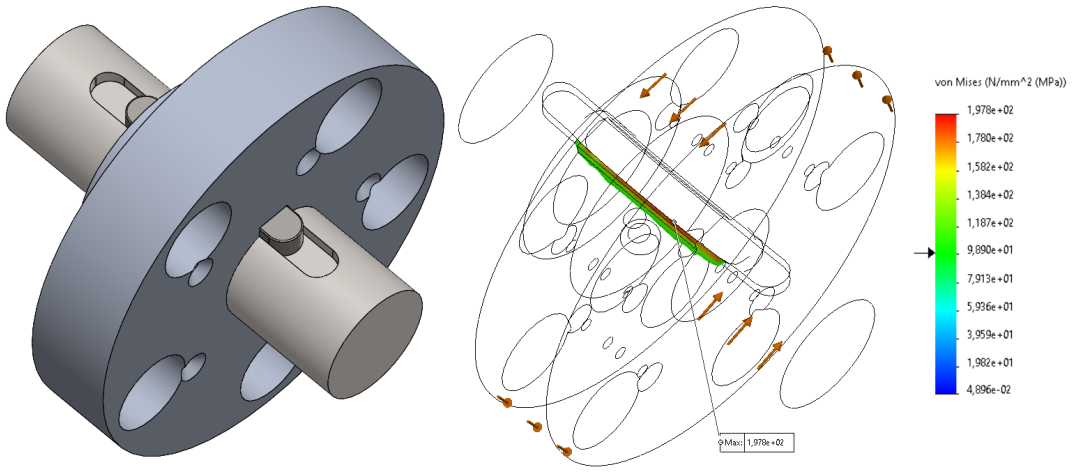


FIGURE 5.6: FEM results of key way analysis with a flange component. The maximum von Mises stress in this study is 197.8 MPa. The iso-clipping image shows only stresses larger than 100 MPa.

The von Mises criterion stress can be directly compared to a material's yield strength, when a material is ductile and isotropic [25]. The yield stress of C45 steel is 500 MPa, resulting in a safety factor of 2.5.

### Fatigue analysis

A fatigue analysis is conducted on the key way to verify the working after a large amount of loading cycles. Fatigue data in the form of an S-N curve taken from the research of A. Lipski [26]. The S-N curve is shown in Figure 5.7.

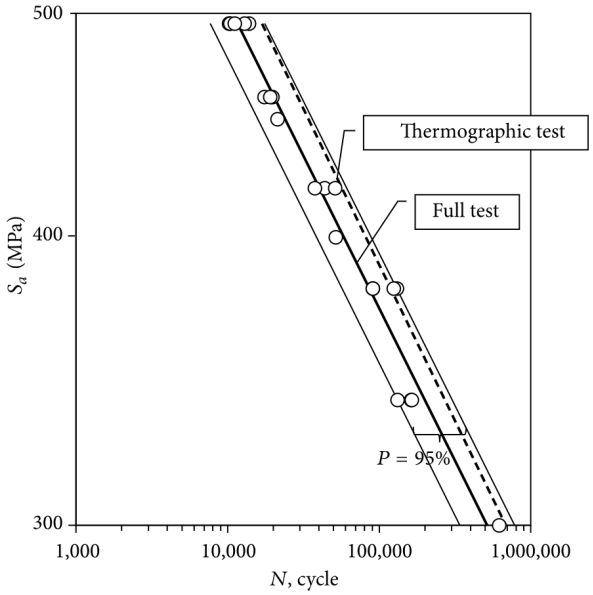


FIGURE 5.7: S-N curve of C45 steel, showing the bending stress in relation to the amount of loading cycles. (image credit: A. Lipski [26])

S-N curves are based on the observed results from testing and show a mean fatigue life for the given material. The S-N curve is used as reference point in the Solidworks software. The software shows that very little damage will occur in the root of the key way, this damage is however inconsequential. The fatigue analysis results in an estimate of a life of more than 2e+07 load cycles.

### Important considerations when constructing axles

When designing axles, there are numerous important considerations, the following points have been drawn up with help of the Roloff/Matek machine book [19].

- Design axles as compact as possible, to reduce the bending moment between pulleys and bearings.
- Place bearings and pulleys as close together as possible to reduce the bending moment in the axle.
- Key ways are not allowed to travel to the edge of a section with increased diameter, this is to reduce the notch effect.
- It is desirable to filet the edges of where the diameter is changing on the axle, to eliminate point stresses.
- Wheels and pulleys must be axially fixed as much as possible, but not with a retaining ring. The grooves needed for retaining rings increase the notch effect. They can be used on the ends of the axle.
- Axles should be axially locked in place but have the possibility to expand due to heating up.

### 5.2.2 Ratchet plate

There are two states of the ratchet plate, one state which transmits power (Figure 5.8a), and one where the ratchet is active, and the axle can rotate freely (Figure 5.8b). The static forces on the ratchet plate in the ratcheting state, are negligible, and only generated by the springs ($< 50N$). In the power transmission state, the forces are significant; therefore a stress analysis is done.

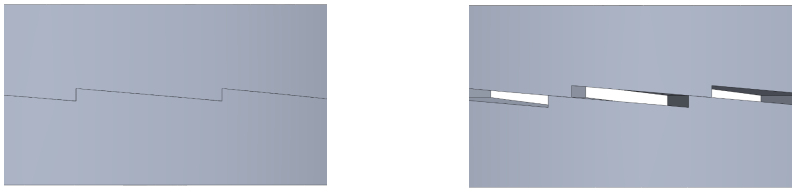

(A) Power transmission state (teeth engaged)

(B) Reverse ratcheting state (teeth rattling)

FIGURE 5.8: Ratcheting states.

The largest torque acting on a ratchet plate in the transmission state is 106.2 Nm, the centerline of the teeth have a radius of 85 mm, which equates to a total load of 1249.4 N on the 20 teeth (62.5 N per tooth). A study using FEM is required due to the complex shape of the ratchet teeth. The material of which the plates are made is 6082-T6 aluminum alloy, which has an allowable yield strength of 250 MPa.

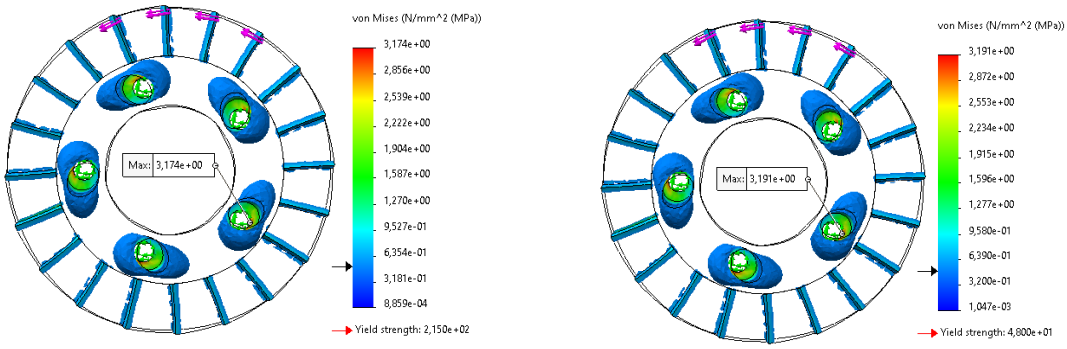


(A) 6082 T6 Aluminum

(B) HP 3D HR PA 12

FIGURE 5.9: FEM study results of the ratchet plate where, in both cases, the von Mises stress does not exceed 3.2 MPa. The aluminum has a maximum deformation of $0.7\mu m$ and the nylon has $28\mu m$ of deformation.

The result of this study is shown in Figure 5.9a. The factor of safety for this part is 79, which is very high. Because of the large factor of safety, a FEM study is also conducted with a Nylon-like material "HP-3D-HR-PA-12", which has an allowable tensile strength of 50 MPa. This material is also investigated because it can be 3D printed in a new way, where the material properties are isotropic. Therefore, FEM analysis can be conducted on these parts. The results of this analysis are shown in Figure 5.9b, the factor of safety with this material is 15.6. The deformation of the aluminum part is $0.7\mu m$ and the nylon part is $28\mu m$. Both of these deformations are acceptable for the prototype AM.

Using 3D printing to produce this part, the process can greatly speed up the geometric development of the ratchet plates, enabling the possibility of an iterative

design process. The size, shape together with the number of teeth can be tested on the prototype.

### Fatigue analysis

A similar mechanism is present in modern bicycles to facilitate the "freewheel" function. A study by T. Mackin. et al. [13] analyzes the fatigue life of a star-ratchet gear (SRG). The study mentions that the number of teeth, a filet in the root of the teeth and a chromium coating can have significant impact on the fatigue life of the teeth.

When conducting a fatigue study on a single tooth of the ratchet plate, the SolidWorks software package shows the message: "Alternating stresses everywhere in the model are below the S-N Curve value, resulting in no damage". This means that the available fatigue data of the "HP-3D-HR-PA-12" material is still greater than the stresses which are occurring in the teeth. This means there will be no fatigue failures of the teeth below $10^6$ loading cycles. The S-N curve fatigue data that was used for this study has been taken from the research of Van Hooreweder [27].

For greater detail and certainty, a FEM study was conducted on a single tooth of the ratchet plate, this can be seen in Figure 5.10. Again, the stresses seen in this analysis are below the threshold where the fatigue data starts, and therefore the ratchet plate can withstand more than $10^6$ loading cycles.

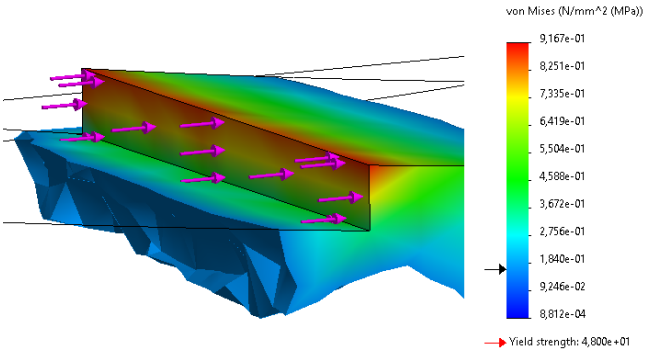


FIGURE 5.10: FEM analysis on a single tooth of the ratchet plate, with a maximum von Mises stress of 0.9 MPa.

### Wear rate

This section is focussed on providing an estimation of the wear on the sliding surface of the ratchet teeth. In an unlubricated wear scenario where there is metal on metal sliding contact, there is no dominant wear mechanism. Adhesive wear calculations can give an indication on the wear of the ratchet plates. Adhesive wear in a steady state equation can be calculated with the Archard wear law [28],

$$V = K\frac{PL}{3H} \tag{5.22}$$

where $V$ is the wear volume $(m^3)$, $K$ is the dimensionless wear coefficient, $P$ is the normal load $(N)$, $L$ is the total sliding distance $(m)$, and $H$ is the Brinell hardness $(kgf/mm^2)$. The specific wear coefficient $(K/H)$ of 6082 aluminum is described by S. Das et al. [29] to be 11e+4 $mm^3/Nm$. This specific wear rate is without lubrication and for an untreated surface. The normal load on the surface is resulting from the springs, which are expected to exert a force of 50 N.

The sliding distance can be estimated using the wave variability of the testing location, there is however no wave data available with the resolution of single waves. The data that the Ocean Grazer company possesses, has averaged out values of waves down to the hour. This data does not include the more detailed wave variability that is required for this estimation. The plates will slide against each other when the trough of the next wave is lower than the current wave.

Since there is no available data for wave variability, a worst-case rough estimate needs to be made. The maximum stroke that can be used in the test setup depends on the wave generator, which is mentioned in Section 4.6.2. The maximum stroke is 1.2 m. When a change of 10% is assumed to happen for every wave, this results in a change of 0.24 m for every stroke. When testing at the highest frequency of 0.2 Hz, over a period of a year this leads to a total change in wave troughs of 757 km. This can be converted to an actual sliding distance of 613 km of the ratchet plates.

Using Equation 5.22 the total wear volume of the two plates is calculated. The result is a wear volume of 11.2e+3 $mm^3$. Assuming that the teeth "jump" a small part of every rattle, the actual contact area can be 80% of the total area of all teeth. The loss of material on the ratchet teeth is expected to be 0.396 mm after a year of full-time running of the test setup in the worst-case scenario. This equates to the teeth being worn down 13.2%.

Lubrication could potentially result in more favorable wear conditions of the ratchet teeth. Moreover, the final design of the AM will be submerged in water, which could have an impact on the wear rate. This needs to be investigated in future research.

#### Production difficulty

Due to the manner in which the teeth interact with each other, the surface shape varies in curvature. This complex topology is needed for the surfaces to run perfectly together. This is comparable to a hypoid gear, the complex shape of a tooth is shown in Figure 5.11.

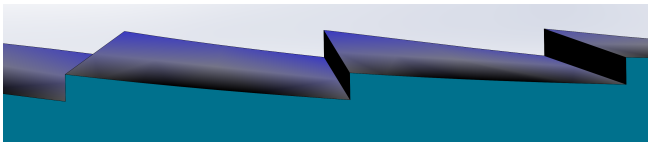

FIGURE 5.11: Image showing the curvature of the teeth. A lighter color represents a greater curvature, and a darker color represents a flatter surface.

Production of this complex shape requires time-consuming and costly 3D machining. This component has been machined by PTB, which is a company in Groningen who specializes in machining. Even with custom tooling built for the production of this component, the surface of the teeth is not ideal. When the teeth slide on each other, the outer tip of the teeth are the only contact point, causing greater wear. This effect can be reduced by increasing the number of teeth.

### 5.2.3 Linear guide

The whole assembly of the linear guide is first studied in a FEM analysis to find the weak components. These components can then be analyzed in more detail in a separate FEM analysis.

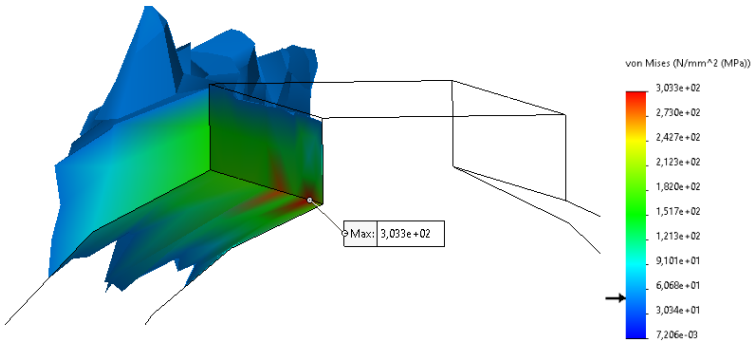


FIGURE 5.12: Von Mises stresses in the Linear flange.

A torque of 106.2 Nm is applied, which is the largest torque acting on these components. Moreover, a linear force of 50 N is applied to simulate the force of the springs. The results of the analysis show that there are no stress concentrations above 50 MPa, which is to be expected as the part is grossly overdimensioned. The only part there the stresses exceed 50 MPa is in the linear flange, as can be seen in Figure 5.12. Here, the stresses are concentrated and have a maximum of 303.3 MPa. Because the concentrated stresses are high in this component, a detailed analysis will be done on the isolated part.

As a result of the geometry of the design, elastic deformation needs to be analyzed to ensure that the teeth of the ratchet plate stay correctly aligned. Imprecise alignment of teeth can lead to slipping of the ratchet mechanism. The deformation can be seen in the FEM analysis and is shown in Figure 5.13.

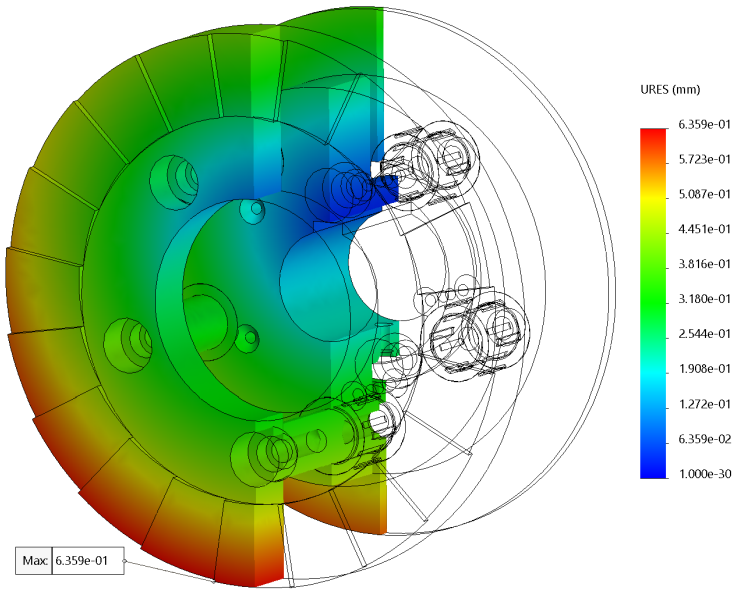


FIGURE 5.13: Elastic displacement in the linear guide assembly, where the largest displacement is 0.64 mm.

When validating the displacement of the teeth of the ratchet plate, the decisive feature is the alignment of the teeth to the other ratchet plate. In a real situation, the applied torque to the ratchet plate will cause it to self center, and distribute the load across all teeth. However, the resulting displacement of the teeth is expected to be 0.64 mm on one side and 0.41 mm on the other side. When doing simple trigonometric calculations, it is found that the misalignment is only 0.07 degrees.

### Linear flange detail analysis

To further investigate the stresses in the linear flange, identical loads are placed on the component as above, 50 N linear force, and 106.2Nm torque. The force of 50 N is, however, added in the area where the springs will exert the force, instead of the whole area. Additionally, due to the complex nature that the torque acts on this component, the torque has been decomposed into components and added to the FEM study as a "remote load". The loads in the simulation can be seen in Figure 5.14a.

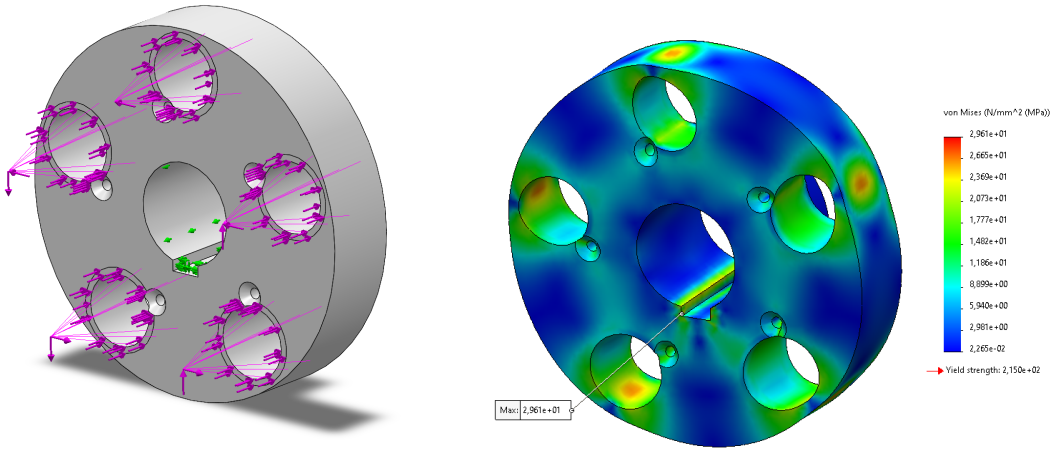


(A) Loads and fixtures in the FEM study of the linear flange.

(B) Results of FEM study on the linear flange with a maximum von Mises stress of 29.6 MPa.

FIGURE 5.14: Linear flange FEM.

The results of this FEM analysis can be seen in Figure 5.14b, where the maximum von Mises stress is 29.6 MPa. This results in a factor of safety of 8.4. The maximum stresses seen in this component are below the threshold of approximately 100 MPa, where fatigue is first observed in 6082-T6 aluminum [30].

## 5.2.4 Pulleys

The pulleys are built out of a single massive block of aluminum 6082-T6. Therefore, it is assumed to be sufficiently strong. For redundancy, A FEM analysis is done to confirm this assumption.

The results of the FEM studies on the pulleys can be seen in Appendix B, where Figure B.1a shows the results of the dynamic pulley, and Figure B.1b shows the results of the floater pulley. The maximum von Mises stresses that are observed are 2.8 Mpa and 32 MPa respectively. To verify the assumption that the pulleys are sufficiently strong, the factor of safety for the dynamic pulley is more than 89 and for the floater pulley is 7.8.

## 5.3 Design recommendations

### 5.3.1 Essence of structural analysis

The structural analysis of the activation mechanism shows that for all parts, the factor is safety is significantly higher than what would be desirable for production purposes. There is an abundance of extra material for every part which can be eliminated to save costs. However, the nature of this design is in a prototyping environment, where different tests are done, parts may be swapped, and loads may be increased in the future. Additionally, when measurements are done concerning the efficiency of the system, deformation of components can lead to errors and inaccuracies.

All the above points considered, the structure is sufficiently strong for the experiments that need to be conducted. Moreover, the additional margin in strength enables the possibility of future upgrades.

### 5.3.2 Design for reliability

When designing the final version of the activation mechanism, key points need to be a priority in the design. Namely, the design needs to be robust and reliable, out in the ocean maintenance is difficult and expensive.

A key component of reliable design is also the robustness in the design. When creating parts that are stronger than they need to be, they will have longer life. Both J. Smith [22] and W. Mulder et al. [21] discuss guidelines for designing for robustness and reliability. The most important parts are summed up:

- Minimize the number of moving parts
- Use only necessary components
- Design with safety margins and overdesign components
- Provide redundancy
- Use materials that suit the conditions that the part will face
- Don't use coated components
- Design robust interfaces

The analysis of reliability can be integrated in the design process, and always run parallel to the design steps. The book of W. Zeiler [31] has a list of important points that will aid the design for reliability (DFR) process. The following tools can be of valuable to the design of the final activation mechanism:

- Modelling of reliability
- Highly accelerated life test (HALT)
- Highly accelerated stress test (HAST)
- Highly accelerated stress screening (HASS)
- Preliminary hazard analysis (PHA)
- Probabilistic safety assessment (PSA)
- Risk potential assessment (RPA)
- Mean time to failures (MTTF) and Mean time between failures (MTBF)
- Event tree analysis (ETA)
- Failure mode and effects analysis (FMEA)

The above-mentioned tools are useful for designing for reliability, but also for assessing the reliability and safety of the system.

# Chapter 6

# Functional analysis

## 6.1 General working principle

The activation mechanism has the goal of being able to engage or disengage the different pistons. This is to vary the pumping power of the pumping system depending on the size of the waves that are passing through. Furthermore, the activation mechanism has to pick up the pistons at the trough point of the wave, ensuring that the maximum amount of power is extracted from the waves.

There are three pulleys on the axle which are attached to pistons, these pulleys can rotate freely on the axle and are only fixed to the axle in a single rotational direction when the piston in engaged. The other direction of rotation will engage the ratchet mechanism. A single pulley attaches the axle to the floater, which provides the floating power from the waves.

### Method of activation

Once a certain combination of pistons need to be activated, the ratcheting mechanism needs to be actuated. There are many approaches which are suitable for actuation. The following methods can be considered for actuation:

- Pneumatic
- Hydraulic
- Electromagnetic
- Electric

The current choice of actuation in the activation mechanism is a pneumatic cylinder with linear guide, the actuator is mounted next to the axle, and pushes against a plate which disengages the ratcheting mechanism. The arm of the actuator has roller bearings which roll on the activation plate when a piston is disengaged. This means that there is always mechanical loss due to friction.

An alternative option which has no moving parts, and can be mounted on the axle, is an electromagnet. Using a magnet to push the ratcheting plates against each other also eliminates the need for springs, considering that magnets have their own spring constant [32].

The only obstacles in using this method of actuation is the power connection to the magnets if they are mounted on the axle. However, due to the low angular velocity and little revolutions that the axle turns, this may be possible to do with a cable which wraps around the axle. Due to the lack of moving parts, this method can be favorable for use in offshore applications, where reliability is of great importance and maintenance needs to be kept to a minimum.

### One-way ratchet

The ratcheting mechanism has the purpose of picking up the pistons at the lowest possible point, which is crucial to extract the most amount of energy from a wave. Every time the trough of the next wave is lower than the current wave, the ratcheting mechanism will ratchet and eliminate the extra height difference. The AM will, however, be controlled on a time interval which significantly larger than the period of the wave. The flaw with the current design of the AM is that the ratchet only works in one direction. If in the period of an hour, the system ratchets multiple times, it cannot return the space to the piston cable. This results in potentially pulling a piston out of the cylinder. To confirm is this is a real problem in the design, testing is needed. It is possible that the ratchet will not rattle if the piston is not at bottom dead center.

### Angle of teeth

It is essential that then the ratchet is activated, that it does not slip in the wrong direction. Empirical testing is needed to verify that this system does not slip. If the system shows evidence of slipping, it needs to be prevented.

This problem can be negated by increasing the angle of the teeth, in a manner where they hook into each other. Increasing the angle of the teeth is shown in Figure 6.1b. Alternatively, stronger springs can be used for pushing the ratchet plates together with greater force, also lessening the possibility of slip.

(A) Perpendicular teeth (B) Angled teeth

FIGURE 6.1: Ratchet plate teeth.

## 6.2 Maintainability

The maintainability of the AM at this stage is not particularly important, the prototype in the water hall is easily serviceable, and will not go through many hours of total work time. On the contrary, the final version will be out in the ocean, and offshore maintenance is not something which is easily conducted. The final version of the AM will need to be designed with the goal of high reliability and minimal maintenance.

The maintenance of a system falls into four categories, where the goal varies. The different types are: Preventive maintenance, Corrective maintenance, Predictive maintenance, and reinforcement. These four different maintenance philosophies are explained in the following points [33].

- **Preventive maintenance** (PM) has the goal of maintaining equipment to a state where it will make it to the next planned service without failing. PM is usually a planned service, to maximize the life of the equipment and minimize breakdowns. This usually includes small oil changes, adding grease and making small adjustments.

- **Corrective maintenance** (CM) is used when equipment has broken down and needs to be fixed again. This many times includes rebuilding and replacing components. Often, damaged components can lead to larger damage to the whole system.
- **Predictive maintenance** is to replace components when before they are expected to break down. With modern advances in computing power, the breakdown of bearings can be predicted precisely using vibrations.
- **Reinforcement** is used when equipment is not functioning properly and needs to be modified to work.

The required maintenance of equipment can be minimized when designed properly. A book has been written by Mulder et al. [21] which gives guidelines for designing for maintainability and reliability. The guidelines which are most relevant for the AM are listed below.

- Use materials that do not prolong maintenance activities.
- Use standard, universal applicable components.
- Provide sufficient space around the maintenance points.
- Guarantee safety by the design itself.
- Design modular.
- Design the weakest link.
- Position components that often need to be maintained at an easily accessible place.

All points described above are focussed on design that prevents failure and minimizes the maintenance. For the final version of the AM, it is desirable to evaluate the bearings and ratchet mechanism from a distance. Roller bearings can be diagnosed with the use of vibrations [34]. Moreover, B. Polok et al. [23] use acoustics to diagnose a ratchet mechanism of a bicycle. Both of these options can be very beneficial to the predictive maintenance of the AM. The lower rotational speed of the AM could be an issue for these measurement techniques, as they both evaluate vibrations and acoustics, which might not be measurable at lower rotational speeds.

## 6.3 Safety

There are two different aspects of safety in the system. First and foremost, safety of humans, this needs to be the priority in the prototype and water hall. The safety of humans which are working on or are close to the system is important but not within the scope of this thesis. It will need to be assessed and guaranteed separately. It is, however, important that the failure modes of the AM will need to be evaluated and should not pose safety threats.

The second safety aspect is the safety of the system and equipment. When a component of the system breaks down, it should not lead to a catastrophic failure, damaging the rest of the equipment and setup. An example could be that the strap attaching the AM to the piston breaks. This would result in the piston crashing through the check valve and destroying the system.

### 6.3.1 Failure mode and effect analysis

For meticulous evaluation of the risks and safety concerns in the system, a structured analysis needs to be carried out. The components, assemblies, and systems need to

TABLE 6.1: Scoring and actions.

| Score | Required actions |
|---|---|
| R < 20 | Limited and acceptable risks |
| 20 < R < 70 | Consideration required |
| 70 < R < 200 | Action required |
| 200 < R < 400 | Immediate action |
| R > 400 | Halt activities |

be thoroughly analyzed for possibilities of failures, and the effects thereof. A failure mode and effect analysis (FMEA) can be conducted. This is a structured method of analyzing systems and components for failure modes, root causes and effects [35] [31].

A FMEA analysis works by first making a list of all the components and their respective failure modes. Each failure mode is then rated numerically to a specific severity. The potential causes are then listed, and the likelihood is given a numerical value, respectively. The final assessment is the design controls for preventing failures and a rating of detectability. The product is taken of the three numerical values. This product is the priority rating and can be scored in Table 6.1, where the required action is found.

The FMEA analysis of the activation mechanism can be found in Appendix C. Table C.1 shows the full analysis respective to each failure mode. Table C.2, C.3 and C.4 show the criteria which are used for the evaluation of severity, probability, and detection respectively.

For all numbers in the risk priority column (RPN) that are above the threshold of 70, an action is described which can be executed to mitigate the risks of failure. This is the output of the FMEA analysis. Ideally, FMEA studies will be repeatedly conducted throughout the development and construction, every time building upon the previous safety measures. The important points that require attention for the first design iteration of the AM are listed below.

1. **Control electronics**
2. **Pneumatic system**
3. **Ratchet mechanism**
4. **Supporting subassembly (frame)**
5. **Actuation components**
6. **Electrical system**

The list is given in order of descending priority, and all points are discussed with a score of over 100 points. The next section will focus on providing adequate safety features and components.

### 6.3.2 Required safety features

From the FMEA analysis, the components with the highest risk potential require fitting safety features.

The first component, **1. Control electronics** has the following output from the FMEA: "Develop a smart safety system to approve and time switching moments." This means that within the electronics that switch the AM from state to state, there has to be a baseline safety feature. This will assess the switch request, and if required, block the deactivation of pistons when they pose a safety hazard.

The second component, **2. Pneumatic system** has the FMEA output of: "Use a pressure regulator and flow regulator." The safety hazard that is caused by the pneumatic system can be mitigated by controlling the flow and pressure in the system. Moreover, it is essential that high-quality components are used where it matters, e.g., air hoses.

The next component, **3. Ratchet mechanism** has the output of: "Extensive testing and powerful springs." This has the goal of preventing slip, which can be dangerous. The probability that slip will occur is very hard to estimate without testing. When the prototype is assembled, it is therefore important that the grip of the ratcheting mechanism is thoroughly tested, and if required, stronger springs can aid in preventing slip.

The fourth risk priority component, **4. Supporting assembly** has a FMEA output of: "Rigid structure with reinforcements." There are significant consequences when this structure is not strong enough and fails. The construction has to be structurally analyzed, and testing is needed with a greater load than required.

The next risk factor is **5. Actuation components**, where the FMEA suggests to: "Control switching via control electronics." The solution to this, falls in line with the solution of the first component, that the electronics need to have a built-in safety baseline. Furthermore, when doing maintenance to the system, it should be powered off completely.

The final risk factor is the **6. Electrical system**, with the FMEA providing the advice: "Grounding of metal components and 24V system." The electrical system needs to be built at a working voltage that sufficiently powers all components, but poses no risk to humans operating the system. Grounding of all metal components is required in the whole setup.

All safety features that are listed above are important for not only the operators of the system, but also as a safeguard to protect the testing setup itself. Additionally, an emergency stop should be implemented in the system. This requires a smarter system than a power down function, as this can lead to pistons being deactivated and crashing.

# Chapter 7

# Efficiency analysis

## 7.1 Energy loss in the activation mechanism

The efficiency of the activation mechanism needs to be evaluated. This includes the system as a whole, and additionally the subcomponents of the activation mechanism. The efficiency can be described as

$$\eta = \frac{P_{in}}{P_{out}} \tag{7.1}$$

where $\eta$ is the efficiency, $P_{in}$ is the total power going in to the system and $P_{out}$. With this concept, different components and subcomponents of the pumping system can be analyzed. The ingoing and outgoing power can be measured at different locations in the system to isolate components and their energy losses.

### 7.1.1 Scope

The entire pumping systems has many subcomponents and sections where energy may be lost. However, the efficiency is limited to only the components of the activation mechanism such as the bearings, pulleys and actuators. Moreover, the efficiency analysis is based on analyzing the efficiency of the AM prototype. The final design of the AM will operate in under different conditions and will need to be analyzed differently. Components submerged in a viscous fluid will also experience surface friction due to hydrodynamic drag.

### 7.1.2 Loss factors

Losses in the system occur in different manners. First, losses which are a result of bad design. When tolerances are too tight, or when bearings are not aligned properly, friction is potentially higher than necessary. Tolerances need to be correct and sliding surfaces and bearings need to be checked for correct alignment. Measurements of ingoing and outgoing power will be useless if there is an additional and avoidable source of friction [36]. The possible sources of friction in the AM are listed as:

- Misaligned bearings
- Faulty lubrication
- Unbalanced axle
- Bad tolerances

The other type of losses in the system are a result of natural friction in bearings, or sliding surfaces. These sources can be minimized in the future, but in most cases not eliminated without altering the design. These sources of friction are listed below.

- Bearings
- Sliding surfaces
- Roll up on pulleys
- Elastic deformation of components
- Electronic power used by electronics and actuation

Test testing methods focus on determining which components have what losses. This does not include the losses of misaligned bearings of bad design, and therefore they should be eliminated as much as possible.

## 7.2 Required information

Losses will need to be determined for all components in the system. For some components like the bearings, this will be determined analytically. For other components which are not possible to determine analytically, empirical testing is needed. The total of all losses can be added up and compared to the number which is resulting from empirical testing of the whole system, providing redundancy in the measurements.

### 7.2.1 Loss in bearings

Bearings are made to minimize friction and wear with rotating components. Friction will however never be eliminated. The power loss of bearings can be calculated by finding the energy loss from the frictional moment of the bearings. The power loss can be calculated with

$$P_{loss} = 1.05 \cdot 10^{-4} Mn \tag{7.2}$$

where M is the total frictional moment $(Nmm)$ and n is the rational speed $(r/min)$. Here, the frictional moment can be calculated with

$$M_{fric} = \mu P \frac{d}{2} \tag{7.3}$$

where $\mu$ is the frictional coefficient which depends on the bearing type (from Table D.1 in Appendix D), P is the load on the bearing $(N)$ and $d$ is the nominal bore diameter of the bearing $(mm)$. To find the efficiency, this power loss needs to be compared to the total power going into the bearing or set of bearings using Equation 7.1. Values of the bearings in the system are approached in the next few sections.

Bearing manufacturer, SKF, has an online tool [37] for looking up the frictional moment and power loss for each type of bearing. As the bearings used in the production of the prototype are of this brand, the SKF tool will provide a good estimation of the losses associated with each bearing. The variables that are entered in the tool are listed below for each single bearing. Temperature is assumed to be the same for all tests, a room temperature of 20 degrees Celsius.

**Main bearings:** The bearings that are used for supporting the main axle is the type: 208-2Z. The angular velocity is 13 rpm with a radial load of 0.644 kN. The resulting frictional moment and power loss of this bearing in normal use is:

$$M_{fric} = 10.9Nmm$$
$$P_{loss} = 0.015W$$

**Pulley bearings:** Every pulley is supported by two bearings with the type: 16008. The angular load is 13 rpm with a radial load of 0.635 kN. The resulting frictional moment and power loss of this bearing in normal use is:

$$M_{fric} = 14Nmm$$
$$P_{loss} = 0.019W$$

**Actuator bearings:** The ratcheting mechanism is activated by three small bearings with the type: 635. The angular velocity is 126 rpm with a radial load of 0.0167 kN. The resulting frictional moment and power loss of this bearing in normal use is:

$$M_{fric} = 0.15Nmm$$
$$P_{loss} = 0.002W$$

#### Total bearing loss

All these losses can be added up, counting all the bearings in the system. This gives the worst-case loss in the bearings of the system, if they are all functioning simultaneously.

TABLE 7.1: Power loss in bearings.

| **Bearing** | **Amount** | $P_{loss}(W)$ | **TOTAL (W)** |
|---|---|---|---|
| Main bearings (208-2Z) | 3 | 0.015 | 0.045 |
| Pulley bearings (16008) | 6 | 0.019 | 0.114 |
| Actuator bearings (635) | 9 | 0.002 | 0.018 |
| | | **TOTAL** | **0.177** |

The losses for the bearings are shown in Table 7.1. The total energy loss due to the bearings is expected to be 0.177 W, under ideal conditions. The efficiency of the system can then be calculated based on an operation power range of 12.97W to 259.4W. This range is based on varying the rotational velocity of the activation mechanism. The efficiency comes out to a range of 98.64% to 99.93%. Lubrication, and assembly, can have a negative influence on this number.

## 7.3 Test plan

This section aims to describe the components that need to be tested and the method of testing. The testing goal is to provide an understanding of the losses that the AM generates, moreover to find the origin of the losses.

In Section 7.1.2 all the sources of friction and power loss are listed. Before testing commences, the assembly of the AM needs to be verified to check if there are misaligned bearings, faulty lubrication, an unbalanced axle or bad tolerances. These variables need to be eliminated as much as possible, that way the measurements as accurate as possible.

The scope of this thesis focuses on only the activation mechanism, where the input is a force in a cable, and the output is another force in three other cables. Figure 2.2 shows the exact scope of this thesis. For testing the efficiency of the entire activation mechanism, a plan is devised. The AM consists of three identical actuation

assemblies, one for each cylinder. Because they are identical, only a single actuation assembly is to be analyzed. The testing method should be organized as follows:

- **TEST A:** Without the AM: hooking the wave generator directly up to the middle piston.
- **TEST B:** With the AM, having only the middle cylinder attached and engaged.
- **TEST C:** With the AM, having only the middle cylinder engaged, but having the other two cylinder attached and disengaged.

For every test, it is important to measure the input force generated by the wave generator, the output force between the AM and the piston, and finally the pumping volume for every test. Comparing the results from these three tests will provide the energy losses of the activation mechanism's main bearings, but also the energy losses that are associated with the actuation components. Measuring the pumping volume is essential to verify that there are no changes in yield.

### 7.3.1 Control variables

For these tests to be valid, certain variables need to stay constant and need to be monitored. These are control variables that could have an influence on the three measurements. For the pumping volume to remain constant, the following items need to be monitored:

- **Temperature** must remain 20 degrees in the water hall, as changes in this could affect the pumping volume by a significant amount.
- **Piston rings** must be measured before and after testing, to verify that there is no additional fluid leaking past the piston as the tests progress.
- **Angular velocity of the wave generator** needs to be kept constant through all series of tests. Alternatively, every test can be run at a multiple of different wave types to investigate if different waves have an effect on the efficiency.
- **Piston straps** need to stay the same, to ensure that the strain remains constant.

### 7.3.2 Equipment

This section describes the sensors and data acquisition hardware that is required for the testing of the activation mechanism. The equipment that is mentioned in this section is based only on the testing of the efficiency of the AM. The pumping system in the water hall likely requires additional testing equipment for the analysis of other components and the system as a whole.

#### Sensors

**Force measurement** The sensors that are required for conducting the tests mentioned in Section 7.3 are proposed in this paragraph. The three variables that need to be measured are the input force to the activation mechanism, the output force from the activation mechanism, and the total pumping volume of the system.

The input and output force can be measured with load cells, which utilize strain gauge sensors. The input and output force, according to Section 5.1.3 is expected to be 2077 N and 1270 N respectively. A load cell must be chosen with a sufficient

capacity. For use in the largest cylinder, and in the input cable, the following load cell can be used: "Tedea Huntleigh Wire Lead Load Cell - model 616". This load cell has a capacity of 500 kg.

**Flow measurement** For measuring the pumping volume of the system, a flow sensor is required. The flow rate is assumed to be larger than conventional sensors. For a large flow rate like this case, sensors are expensive, and in short supply. Alternative methods of measuring flow can be with use of a pitot tube, or by measuring the time it takes to fill up the higher reservoir.

A pitot tube, despite being a great alternative, is likely not accurate enough [38], and not suitable because the flow is not steady state, constantly varying due to the linear pumping motion of the system. The alternative method of measuring the flow is to do timed testing runs, and measuring the difference in volume in the upper and lower reservoir. This can be done by closing the outflow valves. It could, however, be desirable to install a pitot tube anyway, depending on what other tests need to be performed in the testing setup, and what accuracies can be achieved.

#### Data acquisition

In the thesis of M. van Rooij [39], the data acquisition hardware is selected and installed. M. van Rooij uses a BNC terminal block together with a PCI-6036e DAQ board. Since this hardware is already present and not in use at the water hall, this can be reused with the new testing setup. The DAQ board converts the analog signal that it receives from the sensors into a digital signal, that can be read out by a PC. The output resolution is 16 bits, and the input voltage range is $\pm 10$ V.

## 7.4 Losses when submerged in viscous fluid

The design of the AM that is analyzed in this thesis, is meant to function in dry conditions, outside the water. The final version will, on the other hand, work underwater. A functioning version of the AM submerged brings not only complexity to the mechanical design and bearing sealing, but also additional friction.

The shaft will be rotating underwater, meaning that the surface of the rotating parts will experience a surface drag. This surface drag will cause a loss of energy and have a large impact on the overall losses of the AM. The current AM will not have the possibility to test this surface drag. Additionally, the bearings required for functioning in a submerged environment could produce more friction due to the sealing technology. These are two points which need to be further investigated before a final design can be produced.

# Chapter 8

# Discussion

## 8.1 Structural results

The structural analysis of the AM focussed on validating the strength and rigidity of the most critical components. There are a variety of loads on the system, with all three pistons engaged, the largest possible load is achieved. The structural validation was conducted while assuming the worst-case load conditions.

The axle experiences many torsional and bending moments, a manual computational in done and has been validated with a diameter of 37.5 mm, resulting in a FOS of 12.5. The axle has an actual dimension of 40 mm, although the smallest diameter is 37.5 mm. Therefore, the manual calculation focussed on the smaller dimension. A FEM analysis is subsequently conducted on the full geometry of the axle, indicating that the main shaft is sufficiently strong, and the results were comparable to the manual calculation. The FEM analysis did indicate minor stress concentrations in the key slot of the axle. Accordingly, the key slot is also analyzed using FEM. The axle is a rotating body, meaning that it is subject to cyclic loading. To verify the resistance to fatigue, a FEM fatigue analysis has been conducted and approves the axle for 2e+07 loading cycles.

The ratchet plate is responsible for transferring the torque resulting from the pulleys, into the axle. The material used to manufacture these components is 6082-T6 aluminum, having an allowable yield strength of 250 MPa. The FEM analysis on these components shows a maximum von Mises stress of 3.2 MPa, resulting in a FOS of 79. This large FOS brings the opportunity to manufacture with different materials. A new 3D printing technology allows for creating parts with isotropic structural properties. FEM analysis on this material shows that it is sufficiently strong for use in the ratchet plate with a FOS of 15.6. Using this material, different combinations and teeth geometries can be tested and iterated. Due to the low loads on this component, fatigue failure is ruled out. The wear is calculated under extreme usage conditions and without lubrication. This results in a wear of 0.396 mm after a year of full-time operation. A wear case like this is unlikely to exist in the real world. However, it is something which needs to be monitored closely in the final design.

The linear guide and linear flange are crucial to the performance of the ratcheting mechanism, this is why a FEM analysis is conducted on both these components. The linear guide sees a maximum stress of 50 MPa, resulting in a FOS of 5. There is however a larger stress in the key slot of the linear flange, warranting the need of an additional analysis. The largest misalignment due to deformation of the linear guide is expected to be 0.07 degrees, which is non-significant. The detailed FEM analysis of the linear flange results in a FOS of 8.4, having no stresses larger than 29.6 MPa.

A FEM study on the pulleys shows a maximum von Mises stress of 2.8 Mpa for the dynamic pulley and 32 MPa for the floater pulley. The FOS for the two are more than 89 and 7.8 respectively.

Finally, Section 5.3 of the chapter describes important points to consider when designing the final version of the AM. These points are a list which is expected to be of importance to the reliability and robustness of the system's final design.

A key takeaway point from the structural analysis of the AM, is that all parts are grossly overdimentioned, all having a FOS of 5, and many times higher. This is unusual and too strong for the application. It is, however, not necessarily a bad characteristic due to the nature of this specific design. The testing environment of the current design of the AM means that it will see many tests and be part of many higher level system tests. The extra strength allows for a more accurate prediction of losses in the system because no energy and yield is lost due to deformation. additionally, the extra strength facilitates any potential upgrades to the wave generator, allowing for more power and loads.

## 8.2 Functional results

The functional analysis focussed on the working principle of the AM, and discussed the maintainability and safety of the system. A key feature which needs to be investigated further, is the angle, and production method of teeth, these two factors have a major influence on the ratcheting function, and the production costs of the AM.

The maintenance of the final design is an important design goal. The design can be greatly improved for offshore applications, where maintenance is difficult. The design can be altered to use "split-bearings", which allows the axle to be removed radially. With this, a whole AM system can be replaced, and the broken mechanism can be overhauled on shore. Additionally, acoustics can be used to diagnose the ratchet mechanism for wear and failure.

The FMEA study resulted in the precondition of several safety features in the water hall, these features should be installed before major testing happens. Control electronics need to be grounded, and ensure that the activation can only take place when certain conditions are met. The pneumatic system needs to be pressure- and flow regulated. Finally, to ensure the proper functioning, the supporting assembly, ratchet mechanism and actuation components need to be thoroughly tested before operation under full load.

## 8.3 Efficiency results

The efficiency analysis consists mostly of a test plan for further research, where different testing methods are discussed based on what information is needed. The energy losses that are generated by the different bearings are estimated using a tool from SKF, and results in a loss of 0.177 W in the worst-case scenario. This results in an efficiency of 98.64% - 99.93%. However, when the AM is not assembled correctly, the losses can increase due to misaligned bearings. The three main tests that need to be done to evaluate the efficiency of the AM, are the following:

- **TEST A:** Without the AM: hooking the wave generator directly up to the middle piston.
- **TEST B:** With the AM, having only the middle cylinder attached and engaged.
- **TEST C:** With the AM, having only the middle cylinder engaged, but having the other two cylinder attached and disengaged.

Here, for every test, the ingoing force, outgoing force and volume flow of the water needs to be measured. The data can be collected by hardware and software that is already present from previous experiments in the water hall.

## 8.4 Limitations

The research that has been done for this research is based only on the AM that has been designed for the testing setup in the water hall. The main purpose of this design is to undergo and facilitate tests. Limitations arise since this research only focuses on the testing version of the AM. The following points are important limitations of this thesis.

- **Only focussed on the testing version.** This research is only focussed on the design of the testing version of the AM. Whilst recommendations are given for the final design, no direct decisions have been made in this regard.
- **No empirical testing data.** The main reason why testing is needed is to empirically verify the energy losses that occur in the AM. One of the research questions was purely focussed on this matter. Whilst no testing has happened, a test plan has been created describing which tests need to be done and what needs to be measured. Testing the functioning and efficiency of the AM is crucial before a final design is made.
- **Testing AM is not submerged in water.** The final version of the AM will be submerged in the upper reservoir of the pumping system, which adds friction and required a different type of bearing.

## 8.5 Recommendations

### 8.5.1 Design for robustness

When constructing axles that will encounter many rotations and loading cycles, there are several points that should be taken into consideration. This list of points is described in Subsection 5.2.1.

When further iterations of the ratchet plate are designed, the Nylon-based material “HP 3D HR PA 12" can be used for the production. It can be 3D printed and is sufficiently robust for testing and iteration purposes.

Finally, when designing for reliability and robustness, the items mentioned in Subsection 5.3.2 need to be taken into consideration. These provide important guidelines for designing and testing tools for analyzing the robustness of components.

### 8.5.2 Design for maintainability

When designing a system for maintainability, there are many approaches one can take. For the final design of the AM it is important to find a way that broken-down systems can be fixed easily, qualitatively and cost-effective. The whole axle could be quickly swapped out with a new one when using split bearings. This allows for the possibility to do the real maintenance on shore, and offshore just replacing the entire mechanism. Section 6.2 provides a list of important points that should be taken into consideration when designing the final AM.

### 8.5.3 Safety features

The results from the FMEA study showed that the greatest risk to the system is the pistons crashing down the cylinders and through the check valves. This can be due to an incorrect deactivation, or wear on the attachment straps. This needs to be safeguarded to ensure that there are no hazards for humans and no danger to the setup.

## 8.6 Future work

The next big step is to finish the assembly of the AM, and do empirical testing. This will give more insight into the energy losses and functioning of the system. This information is essential to the Ocean Grazer project and its continuity.

Whilst not all crucial, there are many other features and components of the system that require more research. The following list shows points that could provide additional information on the functioning, efficiency or future application of the activation mechanism.

- Empirical testing of the functioning and efficiency of the AM. A testing plan for this can be found in Section 7.3.
- Investigate the possibility of acoustic and vibrational diagnosis of the components of the AM, and verify that it will work with lower rotational speeds. More information about the methods are described by B. Polok et al. [23] and C. Johnson [34].
- The possibility of an electromagnetic actuation system without moving mechanical parts can be investigated to improve the functioning of the AM.
- The wear conditions of the ratchet teeth need to be evaluated for working submerged in water. There could also be an opportunity to implement replaceable teeth in the ratchet plates when wear is high. Additionally, the geometry of the teeth can be optimized for production.
- When testing with this version of the AM is finished, it can be submerged in water to evaluate the energy losses due to surface friction from water.

# Chapter 9

# Conclusion

The initial plan of this thesis was to analyze the design of the AM analytically, and do efficiency testing empirically. Unfortunately, due to the effects of the coronavirus and major delays in the manufacturing of the components, this was not possible. The thesis has therefore been conducted analytically, analyzing the design for robustness, reliability, and maintainability. A test plan has been created for the empirical analysis of the efficiency.

The structural analysis showed that all components of the AM are not only sufficiently strong and robust, but very overdimentioned. The lowest factor of safety in the components is a factor of 5, leaving enough margin for upgrades and changes to the testing setup. The ratchet plate has, in the most extreme case, without lubrication, a wear of 0.396 mm per year. The ratchet plate has a fatigue life of at least 1e+06 loading cycles, and the axle is expected to have a fatigue life of more than 2e+07 loading cycles.

The functional analysis described other methods of actuation, which could be an improvement to the final design, as it could potentially eliminate many moving parts. The one-way ratchet could cause a situation where the pistons are pulled out the top of the cylinders, this is however not confirmed as a problem and will need to be tested when the setup is functioning. Moreover, the angle and surface of the teeth is a complex shape which is difficult and costly to manufacture. There is a list of points which are mentioned in Section 6.2 that can be implemented in the design to improve the maintainability aspect. The last part of the functional analysis provides important safety features which are to be implemented in the testing setup at the water hall.

The efficiency, on which no empirical testing was achievable, has been estimated, and a testing plan has been created. The loss factors are expected to be mainly caused by the bearings in the assembly, and has been calculated to have and efficiency of 98.64% - 99.93%. The testing plan introduces three tests which are to be conducted to empirically verify the energy losses of the AM.

# Bibliography


[1] IEA. "World Energy Outlook 2019". In: (2019). URL: https://www.iea.org/reports/world-energy-outlook-2019.

[2] IEA. *Global electricity demand by region in the Stated Policies Scenario, 2000-2040*. 2019. URL: https://www.iea.org/data-and-statistics/charts/global-electricity-demand-by-region-in-the-stated-policies-scenario-2000-2040.

[3] Mehmet Melikoglu. "Current status and future of ocean energy sources: A global review". In: *Ocean Engineering* 148 (2018), pp. 563–573.

[4] IEA. *Global electricity generation mix by scenario, 2018, Stated Policies and Sustainable Development Scenarios 2040*. 2019. URL: https://www.iea.org/data-and-statistics/charts/global-electricity-generation-mix-by-scenario-2018-stated-policies-and-sustainable-development-scenarios-2040.

[5] University of Groningen. *Artist impression Ocean Grazer*. https://www.rug.nl/news/2018/10/photo-report_-the-ocean-grazer?lang=en. (Image has been cropped from original). 2018.

[6] University of Groningen. *Ocean Grazer Project*. https://www.rug.nl/research/cmme/ocean-grazer-project. Accessed: 2021-07-30. 2021.

[7] J. Welink. *Creating a scale model design for the ocean grazer project*. University of Groningen. Groningen, NL, 2014.

[8] A. van Driel. "Development of the activation mechanism for the Ocean Grazer". MA thesis. Groningen, NL: University of Groningen, 2017.

[9] M. Abbas. *Eindopdracht M. Abbas*. Alfa College. Groningen, NL, 2015.

[10] L. Hut. "Investigating the dynamic behavior of a multi-piston pump". MA thesis. Groningen, NL: University of Groningen, 2018.

[11] L.J.P. Evers. "Designing a transmission system for the Ocean Grazer". MA thesis. Groningen, NL: University of Groningen, 2015.

[12] VP Bondaletov. "Ratchet mechanisms for high-speed transmissions". In: *Russian Engineering Research* 28.9 (2008), pp. 845–848.

[13] Thomas J Mackin et al. "Fatigue failure of a star–ratchet gear". In: *Engineering Failure Analysis* 32 (2013), pp. 334–347.

[14] Pawan K Goenka. "Dynamically loaded journal bearings: finite element method analysis". In: (1984).

[15] Vasilios Bakolas et al. "A first approximation of the global energy consumption of ball bearings". In: *Tribology Transactions* just-accepted (2021), pp. 1–10.

[16] Shoaib Iqbal et al. "Frictional power loss in solid-grease-lubricated needle roller bearing". In: *Lubrication Science* 25.5 (2013), pp. 351–367.

[17] C Jarzynski and O Mazonka. "Feynman's ratchet and pawl: An exactly solvable model". In: *Physical Review E* 59.6 (1999), p. 6448.

[18] D. Jannasch J.Vobiek H. Wittel D. Muhs. *Roloff/Matek Machine onderdelen - Theorieboek*. Den Haag: SDU uitgevers, 2013.

[19] D. Jannasch J.Vobiek H. Wittel D. Muhs. *Roloff/Matek Machine onderdelen - Tabellenboek*. Den Haag: SDU uitgevers, 2013.

[20] Dana Crowe and Alec Feinberg. *Design for reliability*. CRC press, 2017.

[21] Wienik Mulder et al. "Design for maintenance: guidelines to enhance maintainability, reliability and supportability of industrial products". In: (2012).

[22] Jonathan Smith and P John Clarkson. "A method for assessing the robustness of mechanical designs". In: *Journal of Engineering Design* 16.5 (2005), pp. 493–509.

[23] Bartosz Połok and Piotr Bilski. "Diagnostics of the ratchet mechanism using the acoustic analysis". In: (2020).

[24] "Chapter 1 - The Marine Environment". In: *The Maritime Engineering Reference Book*. Ed. by Anthony F. Molland. Oxford: Butterworth-Heinemann, 2008, pp. 1–42. ISBN: 978-0-7506-8987-8. DOI: https://doi.org/10.1016/B978-0-7506-8987-8.00001-9. URL: https://www.sciencedirect.com/science/article/pii/B9780750689878000019.

[25] Bob McGinty. *Von Mises Stress*. 2021. URL: https://www.continuummechanics.org/vonmisesstress.html.

[26] Adam Lipski. "Rapid determination of the SN curve for steel by means of the thermographic method". In: *Advances in Materials Science and Engineering* 2016 (2016).

[27] Brecht Van Hooreweder and Jean-Pierre Kruth. "High cycle fatigue properties of selective laser sintered parts in polyamide 12". In: *CIRP Annals* 63.1 (2014), pp. 241–244.

[28] Per Møller and Lars Pleht Nielsen. *Advanced surface technology*. Møller & Nielsen, 2013.

[29] Sanjeev Das et al. "Effect of static and dynamic ageing on wear and friction behavior of aluminum 6082 alloy". In: *Tribology international* 60 (2013), pp. 1–9.

[30] A Djebli et al. "A non-linear energy model of fatigue damage accumulation and its verification for Al-2024 aluminum alloy". In: *International Journal of Non-Linear Mechanics* 51 (2013), pp. 145–151.

[31] W. Zeiler. *Basisboek ontwerpen : van 'methodisch ontwerpen' tot 'integraal ontwerpen'*. Nederlands. Noordhoff Uitgevers, 2014. ISBN: 978-90-01-81864-7.

[32] Miroslav Novak, Josef Cernohorsky, and Miloslav Kosek. "Simple electro-mechanical model of magnetic spring realized from FeNdB permanent magnets". In: *Procedia Engineering* 48 (2012), pp. 469–478.

[33] R Keith Mobley. *An introduction to predictive maintenance*. Elsevier, 2002.

[34] Chris Johnson. 2021. URL: https://www.smbbearings.com/technical/bearing-noise-vibration.html.

[35] Cansu Dağsuyu et al. "Classical and fuzzy FMEA risk analysis in a sterilization unit". In: *Computers & Industrial Engineering* 101 (2016), pp. 286–294.

[36] ZS Safar. "Energy loss due to misalignment of journal bearings". In: *Tribology international* 17.2 (1984), pp. 107–109.

[37] SKF. 2021. URL: https://www.skfbearingselect.com/#/size-lubrication/single-bearing.

[38] 2021. URL: https://www.omega.com/en-us/resources/pitot-tube.

[39] M van Rooij. "EXPERIMENTAL VALIDATION OF DYNAMICAL CONTACT MODELS OF THE OCEAN GRAZER". MA thesis. Groningen, NL: University of Groningen, 2015.

# Appendix A

# Shear and bending diagrams

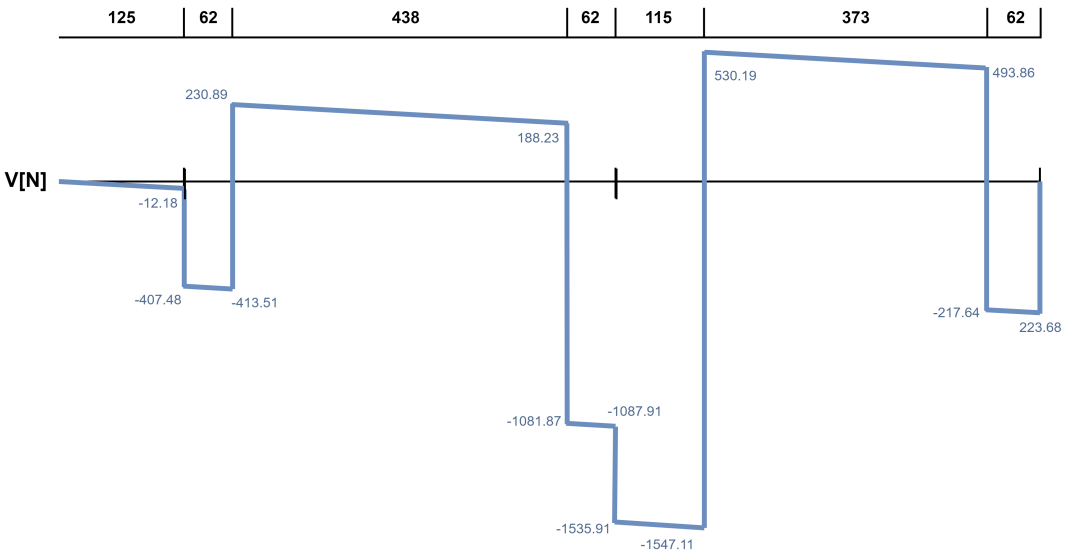


(A) Shear force diagram.

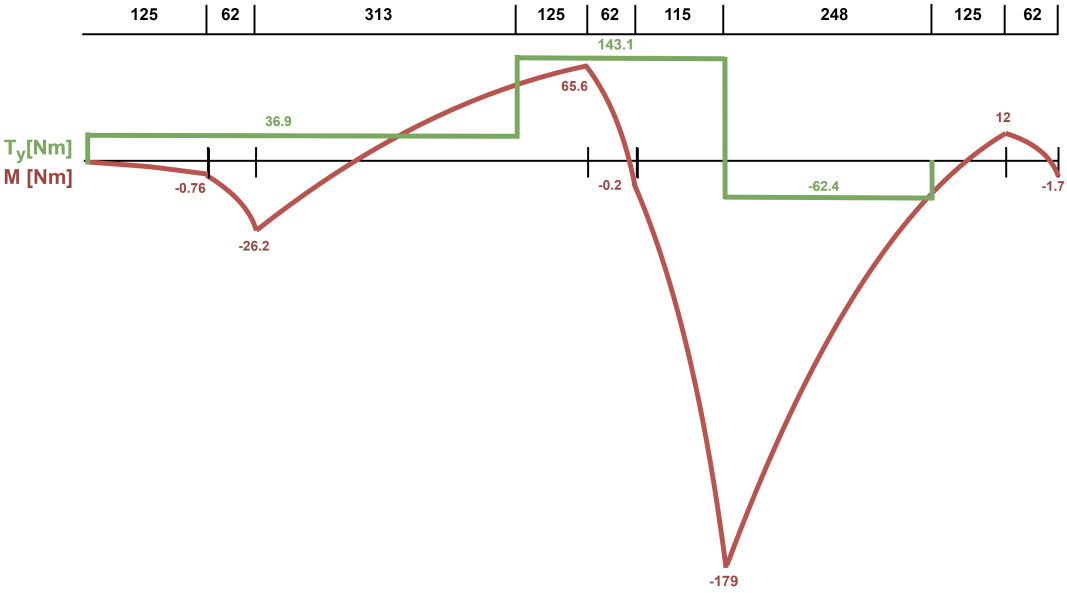


(B) Bending moment diagram and turning moment diagram.

FIGURE A.1: Diagrams of the axle computations.

# Appendix B

# FEM results of pulleys

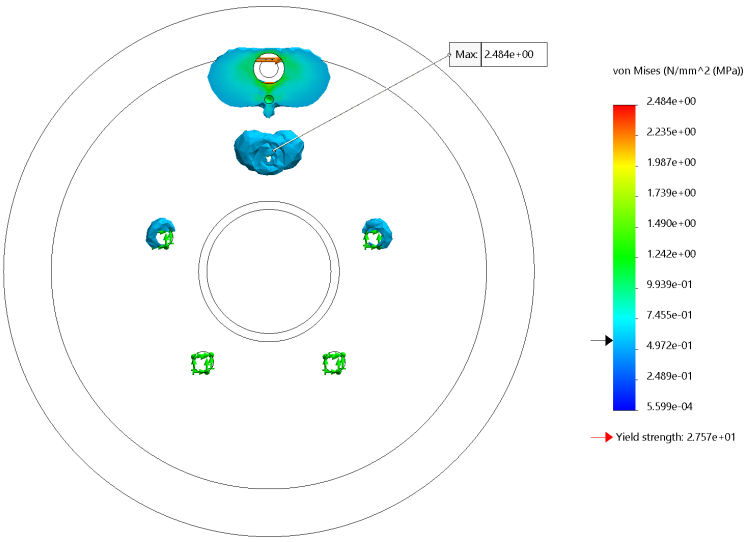


(A) The dynamic pulley with a maximum von Mises stress of 2.8 MPa.

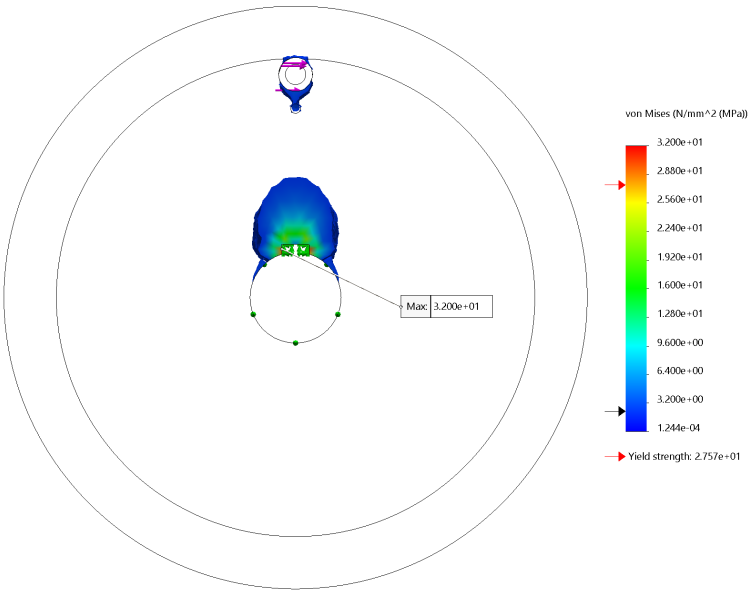


(B) The floater pulley with a maximum von Mises stress of 32 MPa.

FIGURE B.1: FEM studies of the Dynamic- and floater pulley, showing the von Mises stress distribution.

# Appendix C

# Failure mode and effect analysis

TABLE C.1: FMEA worksheet.

| Item / Function | Potential Failure Mode(s) | SEVERITY<br>Potential Effect (s) of Failure | Sev | LIKELIHOOD<br>Potential Cause (s)/ Mechanism (s) of Failure | Prob | DETECTABILITY<br>Current Design Controls | Det | RPN | Recommended Action(s) |
|---|---|---|---|---|---|---|---|---|---|
| **The supporting sub assembly (frame)** | Elastic deformation | Damage to cylinders / stuck pistons | 6 | Design failure or human error | 2 | | 3 | **36** | |
| | Shifting of correct positioning | Damage to cylinders / stuck pistons | 6 | Faulty assembly | 3 | | 3 | **54** | |
| | Fracture of beams | Full catastrophic failure / pistons crashing through check valves | 9 | Design error | 1 | | 1 | **9** | |
| | Fasteners loosening | Full catastrophic failure / pistons crashing through check valves | 9 | Faulty assembly | 3 | Usage of retaining nuts | 4 | **108** | Rigid structure with reinforcements |
| **Roller bearing** | Full seizure | Damage to rattling mechanism and support structure | 7 | Bearings not lined up properly | 3 | | 4 | **84** | Installation of bearings per manufacturer guidelines |
| **Ratchet mechanism** | Losing grip, allowing for free rotation | Pistons falling down, crashing through check valve | 9 | Wrong design or assembly of the mechanism | 5 | Validation of working | 3 | **135** | Extensive testing and powerful springs |
| | Not ratcheting | Seizure of axle | 6 | Faulty assembly or design | 3 | Validation of working | 3 | **54** | |
| | Not engaging | Broken ratchet plate | 6 | Many use cycles, large impact forces | 2 | Test cycles | 4 | **48** | Electronic safety measures |
| **Actuation components** | Accidental actuation | Pistons falling down, crashing through check valve | 9 | Wrong assembly of components | 4 | | 3 | **108** | Control switching via control electronics |
| | Seizure | Unable to operate properly | 6 | Bad lubrication or faulty design | 4 | | 3 | **72** | Extensive testing and adequate lubrication |
| **Wave generator** | Axle breaking | Higher stresses on components | 3 | Seizure of cable, leading to higher stresses on motor | 2 | | 4 | **24** | |
| | Coming off of moment arm | Crashing of the system | 7 | Faulty assembly | 2 | Securing bolt in place | 2 | **28** | |

Table C.1 (Continued)

| | | | | | | | | | |
|---|---|---|---|---|---|---|---|---|---|
| **Connecting cable** | Mechanical failure | Pistons falling down, crashing through check valve | 9 | Bad inspection / wrongful assembly / wrong pulleys | 5 | Testing cycle | 2 | **90** | Use a cable with a sufficient strength and safety factor |
| **Pulleys** | Seizure | Damage to connecting cable | 3 | Bad lubrication / forces too large | 1 | Load testing | 4 | **12** | |
| **Electrical system** | Shorting | Electrical shock to operators | 9 | Wrongful assembly of electrical system | 3 | Full test and grounding | 4 | **108** | Grounding of metal components and 24V system |
| **Pneumatic system** | Activation at wrong moment | Catastrophic failure of pump, danger to humans | 9 | Bad assembly / bad design of system | 3 | Stable control electronics | 3 | **81** | Safety system in the control electronics |
| | Squasing of body parts in components | Human injury | 10 | Human error | 2 | | 2 | **40** | |
| | Rupture of air hose | Rapid deactivation of piston, causing catastrophic failure | 9 | Faulty assembly or old hose | 4 | Test at higher pressure | 4 | **144** | Use a pressure regulator and flow regulator |
| **Control electronics** | Activation at wrong moment | Catastrophic failure of pump, danger to humans | 9 | Human error / Failure of electronic components | 7 | Safety control system | 3 | **189** | Develop a smart safety system to approve and time switching moments |

TABLE C.2: Criteria for severity.

| Effect | SEVERITY of Effect | Ranking |
|---|---|---|
| **Hazardous without warning** | Very high severity ranking when a potential failure mode affects safe system operation without warning | **10** |
| **Hazardous with warning** | Very high severity ranking when a potential failure mode affects safe system operation with warning | **9** |
| **Very High** | System inoperable with destructive failure without compromising safety | **8** |
| **High** | System inoperable with equipment damage | **7** |
| **Moderate** | System inoperable with minor damage | **6** |
| **Low** | System inoperable without damage | **5** |
| **Very Low** | System operable with significant degradation of performance | **4** |
| **Minor** | System operable with some degradation of performance | **3** |
| **Very Minor** | System operable with minimal interference | **2** |
| **None** | No effect | **1** |

TABLE C.3: Criteria for Probability.

| PROBABILITY of Failure | Failure Prob | Ranking |
|---|---|---|
| **Very High: Failure is almost inevitable** | >1 in 2 | **10** |
| | 1 in 3 | **9** |
| **High: Repeated failures** | 1 in 8 | **8** |
| | 1 in 20 | **7** |
| **Moderate: Occasional failures** | 1 in 80 | **6** |
| | 1 in 400 | **5** |
| | 1 in 2,000 | **4** |
| **Low: Relatively few failures** | 1 in 15,000 | **3** |
| | 1 in 150,000 | **2** |
| **Remote: Failure is unlikely** | <1 in 1,500,000 | **1** |

TABLE C.4: Criteria for Detection.

| Detection | Likelihood of DETECTION by Design Control | Ranking |
|---|---|---|
| **Absolute Uncertainty** | Design control **cannot** detect potential cause/mechanism and subsequent failure mode | **10** |
| **Very Remote** | **Very remote** chance the design control will detect potential cause/mechanism and subsequent failure mode | **9** |
| **Remote** | **Remote** chance the design control will detect potential cause/mechanism and subsequent failure mode | **8** |
| **Very Low** | **Very low** chance the design control will detect potential cause/mechanism and subsequent failure mode | **7** |
| **Low** | **Low** chance the design control will detect potential cause/mechanism and subsequent failure mode | **6** |
| **Moderate** | **Moderate** chance the design control will detect potential cause/mechanism and subsequent failure mode | **5** |
| **Moderately High** | **Moderately High** chance the design control will detect potential cause/mechanism and subsequent failure mode | **4** |
| **High** | **High** chance the design control will detect potential cause/mechanism and subsequent failure mode | **3** |
| **Very High** | **Very high** chance the design control will detect potential cause/mechanism and subsequent failure mode | **2** |
| **Almost Certain** | Design control **will** detect potential cause/mechanism and subsequent failure mode | **1** |

# Appendix D

# Bearing types and coefficient of friction

TABLE D.1: A table with the friction coefficients of different types of bearings.

| **Bearing type** | **Friction coefficient** $\mu$ |
|---|---|
| Deep groove ball bearing | $0.0010 \sim 0.0015$ |
| Angular contact ball bearing | $0.0012 \sim 0.0020$ |
| Self-aligning ball bearing | $0.0008 \sim 0.0012$ |
| Cylindrical roller bearing | $0.0008 \sim 0.0012$ |
| Full complement type needle roller bearing | $0.0025 \sim 0.0035$ |
| Needle roller and cage assembly | $0.0020 \sim 0.0030$ |
| Tapered roller bearing | $0.0017 \sim 0.0025$ |
| Spherical roller bearing | $0.0020 \sim 0.0025$ |
| Thrust ball bearing | $0.0010 \sim 0.0015$ |
| Spherical thrust roller bearing | $0.0020 \sim 0.0025$ |